Quasi-shear waves in the zero-order approximation of the quasi-isotropic approach. Preliminary results [1]

Ivan Pšenčík

Geophysical Institute, Acad.Sci.of Czech Republic, Boční II, Praha 4, Czech Republic; e-mail: ip@ig.cas.cz

ABSTRACT

First results obtained with the zero-order approximation of the quasi-isotropic (QI) approach are presented. The results were obtained with the updated version of the program package ANRAY. The QI results are compared with results obtained by the ray method for inhomogeneous anisotropic media and isotropic media. The results confirm theoretical conclusions that the QI approach represents a link between both ray methods. Presented numerical experiments show that the QI approach can be used in regions with extremaly weak anisotropy including isotropy, in regions in which the two qS waves couple and propagate together as well as in regions, in which the qS waves become decoupled and can thus be, in principle, studied by the ray method for anisotropic media. This is a good news for future applications of the QI approach, in which the QI approach should be combined with the ray methods for isotropic and anisotropic media.

INTRODUCTION

It is well known that the ray method for inhomogeneous anisotropic media yields distorted results for the qS waves propagating in inhomogeneous weakly anisotropic media or in vicinity of qS wave singularities, such as a kiss or an intersection singularity. To avoid these problems, the so-called *quasi-isotropic approach*, see Kravtsov (1968), Kravtsov & Orlov (1980), Červený (1998), Pšenčík (1997, 1998a) was proposed. The basic idea of this approach is to seek the asymptotic solution of the elastodynamic equation as an expansion with respect to two small parameters of the same order: the small parameter used in the standard ray method and a parameter characterizing differences of tensors of elastic parameters of a weakly anisotropic medium and of a nearby "background" isotropic medium. The zero-order approximation of the QI approach is equivalent to the coupling ray theory (CRT), which was proposed by Coates & Chapman (1990) to solve the same problems of the ray method.

[1] Seismic Waves in Complex 3-D Structures, Report 7 (Department of Geophysics, Charles University, Prague 1998)

In this contribution, we concentrate on the zero-order approximation of the QI approach applied to qS waves. The program package ANRAY was modified for this purpose, see Pšenčík (1998b). First, a background isotropic model corresponding to the studied model of a weakly anisotropic medium is specified. Its P and S wave velocities can be found by various averagings of qP, $qS1$ and $qS2$ phase velocities. Rays connecting a source with receivers and several important quantities evaluated along these rays are calculated in the background isotropic medium. Two coupled linear differential equations for the QI amplitudes are then solved along these rays for selected frequencies in the considered frequency range. From the resulting frequency-dependent QI amplitudes, frequency responses are calculated, which are used later for constructions of seismograms and particle motion diagrams corresponding to an arbitrary source signal. In contrast to the formulation proposed by Coates & Chapman (1990), the QI approach does require calculation of neither travel time corrections nor polarization vectors. This makes the QI approach efficient and stable.

In the following, we present qS wave fields in two synthetic VSP experiments. The two experiments differ by considered models. In both cases vertically inhomogeneous weakly anisotropic HTI (transversely isotropic with horizontal axis of symmetry) media are considered. In the first experiment anisotropy is so weak that the medium is effectively isotropic. We compare the QI results with the results of the ray method for anisotropic media (ANI) and of the ray method for isotropic media (ISO). We show that the QI approach yields results predicted by the ray method for isotropic media and differs considerably from results predicted by ANI. In the second experiment anisotropy is considerably stronger than in the previous case but still weak. By varying prevailing frequency of the source signal and comparing results of the QI approach with ANI and ISO, we show that the results of the QI approach resemble results of ISO or ANI depending on the local strength of anisotropy and on frequency. This confirms theoretical observations that the QI approach represents a link between the ray methods for isotropic and anisotropic media.

Let us note that Bulant & Klimeš (1998) developed a code based on the formulation close to the formulation of Coates & Chapman (1990). They present results, obtained for the same model as used in this contribution, in this report.

BASIC FORMULAE

We review here briefly the basic formulae necessary for the calculation of the zero-order approximation of the QI approach.

Let us consider the tensor of density normalized elastic parameters in weakly anisotropic media in the form

$$a_{ijkl} = a^0_{ijkl} + \Delta a_{ijkl}. \tag{1}$$

The parameters a^0_{ijkl} of a nearby background isotropic medium are given by the formula

$$a^0_{ijkl} = (\alpha^2 - \beta^2)\delta_{ij}\delta_{kl} + \beta^2(\delta_{ik}\delta_{jl} + \delta_{il}\delta_{jk}). \tag{2}$$

The symbols α and β denote the P and S wave velocities of the background isotropic medium. The quantities Δa_{ijkl} in (1) denote deviations of elastic parameters of the weakly anisotropic medium from isotropy.

The qS wave Green function in the zero-order approximation of the QI approximation reads

$$G_{in}(\tau,\tau_0,\omega) = e^{i\omega\tau}\Big[\mathcal{B}_n(\tau)e_i^{(1)}(\tau) + \mathcal{C}_n(\tau)e_i^{(2)}(\tau)\Big]. \tag{3}$$

The symbol τ_0 denotes time at the source, $\tau - \tau_0$ is the travel time along the ray of the S wave in the background isotropic medium The vectors $e_i^{(I)}$ are the basis vectors of the ray centred coordinate system. They also represent the polarization vectors of S waves in isotropic media. The terms $\mathcal{B}_n(\tau)$ and $\mathcal{C}_n(\tau)$ are the amplitudes of the qS waves in the zero-order approximation of the QI approach. We express the terms $\mathcal{B}_n(\tau)$ and $\mathcal{C}_n(\tau)$ appearing in (3) in the following form

$$\mathcal{B}_n(\tau) = \frac{\bar{\mathcal{B}}_n(\tau)}{\sqrt{\rho(\tau)\beta(\tau)\Omega_M(\tau)}}, \qquad \mathcal{C}_n(\tau) = \frac{\bar{\mathcal{C}}_n(\tau)}{\sqrt{\rho(\tau)\beta(\tau)\Omega_M(\tau)}}. \tag{4}$$

The symbol ρ denotes the density and the symbol Ω_M denotes a quantity proportional to the relative geometrical spreading $|\Omega_M|$. It can be obtained from the dynamic ray tracing in the background isotropic medium. In contrast to the standard ray method, where the terms $\bar{\mathcal{B}}_n(\tau)$ and $\bar{\mathcal{C}}_n(\tau)$ are constant along a ray, in the zero-order approximation of the QI approach, these terms are frequency-dependent solutions of two coupled linear ordinary differential equations of the first order

$$\frac{d\bar{\mathcal{B}}_n}{d\tau} = -\frac{1}{2}i\omega\beta^{-2}(B_{11}\bar{\mathcal{B}}_n + B_{12}\bar{\mathcal{C}}_n), \qquad \frac{d\bar{\mathcal{C}}_n}{d\tau} = -\frac{1}{2}i\omega\beta^{-2}(B_{12}\bar{\mathcal{B}}_n + B_{22}\bar{\mathcal{C}}_n) \tag{5}$$

with the initial conditions

$$\bar{\mathcal{B}}_n(\tau_0) = \frac{e_n^{(1)}(\tau_0)}{4\pi\sqrt{\rho(\tau_0)\beta(\tau_0)}}, \qquad \bar{\mathcal{C}}_n(\tau_0) = \frac{e_n^{(2)}(\tau_0)}{4\pi\sqrt{\rho(\tau_0)\beta(\tau_0)}}. \tag{6}$$

The initial conditions (6) correspond to a unit force oriented along the coordinate axis x_n. The symbols B_{mn} in (6) denote elements of the weak anisotropy matrix, which plays an important role in formulae related to weakly anisotropic media, see e.g. Pšenčík & Gajewski (1998),

$$B_{mn} = \Delta a_{ijkl}e_i^{(m)}e_j^{(3)}e_k^{(3)}e_l^{(n)}. \tag{7}$$

If the considered medium is isotropic, the formula (3) reduces to formula for the zero-order ray approximation of the Green function in isotropic media. If anisotropy of the medium is strong, inhomogeneity weak and frequency high, the zero-order approximation of the QI approach yields two independent qS waves (Kravtsov & Orlov 1980, Pšenčík 1997, 1998a) and its results converge to results of the ray method for anisotropic media. It is the aim of this contribution to illustrate this fact by synthetic examples.

NUMERICAL TESTS

In the following tests, we shall consider a VSP configuration shown in Fig.1.

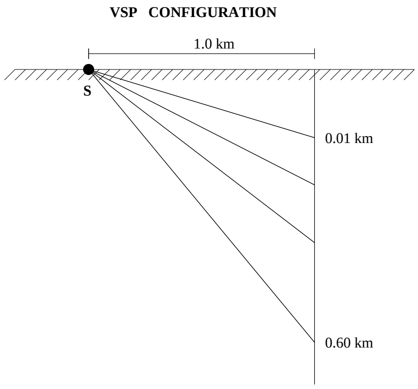

Figure 1

The point source, a vertical force pointing downwards, is situated at the point S, 1 km away from the mouth of the borehole. Neither at the source nor at receivers the effects of the free surface are considered. The windowed symmetric Gabor signal shown in Fig.2 is used as a source-time function. Its prevailing frequency, if not specified otherwise, is 50 Hz.

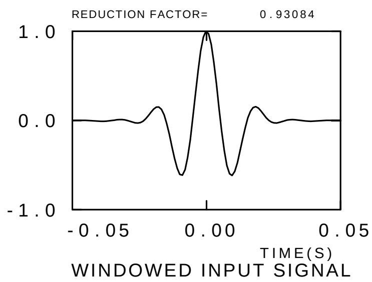

Figure 2

There are 29 receivers in the borehole distributed with equal step of 0.02 km starting at the depth of 0.01 km. The deepest receiver is thus at the depths of 0.57 km. The receivers record vertical (positive downwards), transverse and radial (positive away from the source) components of the S or qS wave field. The recording system is right-handed. resulting seismograms or particle motion diagrams are shown with no scaling between components and traces; real amplitude relations are shown.

Two models of vertically inhomogeneous transversely isotropic media with horizontal axis of symmetry (HTI) are considered. In the first one, taken from the study of Coates & Chapman (1990), anisotropy is extremaly weak. We call this model EWA (extremaly weak anisotropy). Anisotropy of the other, called WA (weak anisotropy) is stronger. In both models, the axis of symmetry of the HTI media is 45^o out of the vertical plane containing the source and the borehole - plane of the experiments.

Model EWA

In a coordinate system, in which the axis of symmetry is parallel to the $x-$axis, the matrices of density normalized elastic parameters, in $(\mathrm{km/s})^2$, at depths of 0.0 km and 1.0 km have the following form

$$\begin{pmatrix} 20.248 & 7.457 & 7.457 & 0.00 & 0.00 & 0.00 \\ & 20.250 & 7.448 & 0.00 & 0.00 & 0.00 \\ & & 20.250 & 0.00 & 0.00 & 0.00 \\ & & & 6.401 & 0.00 & 0.00 \\ & & & & 6.386 & 0.00 \\ & & & & & 6.386 \end{pmatrix}$$

and

$$\begin{pmatrix} 30.878 & 11.372 & 11.372 & 0.00 & 0.00 & 0.00 \\ & 30.881 & 11.358 & 0.00 & 0.00 & 0.00 \\ & & 30.881 & 0.00 & 0.00 & 0.00 \\ & & & 9.762 & 0.00 & 0.00 \\ & & & & 9.739 & 0.00 \\ & & & & & 9.739 \end{pmatrix}.$$

The elastic parameters between the depths of 0.0 and 1.0 km are determined by linear interpolation. The density is constant throughout the model and equals 1.0 $\mathrm{g/cm^3}$. Sections of the qS wave phase velocity surfaces by the plane of experiment at the depths of 0.0 and 0.6 km are shown in Fig.3.

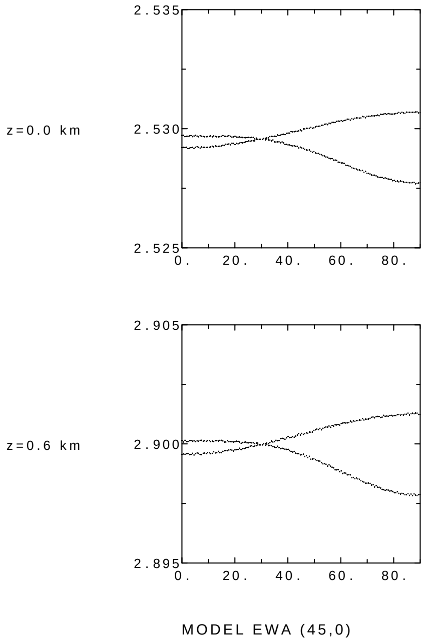

Figure 3

The vertical axes show phase velocity, horizontal axes angles. The angle 0^o corresponds to horizontal propagation, the angle 90^o to vertical propagation. We can see that the model is not only extremaly weakly anisotropic but it also contains a crossing singularity for angles around 30^o. Anisotropy in the above sections $((c_{qS1} - c_{qS2})/c_{aver})$ varies from 0.02% for horizontal propagation to 0.1% for vertical propagation.

Model WA

In a coordinate system, in which the axis of symmetry is parallel to the $x-$axis, the matrices of density normalized elastic parameters, in $(\mathrm{km/s})^2$, at depths of 0.0 km and 1.0 km have the following form

$$\begin{pmatrix} 13.39 & 4.46 & 4.46 & 0.00 & 0.00 & 0.00 \\ & 15.71 & 5.04 & 0.00 & 0.00 & 0.00 \\ & & 15.71 & 0.00 & 0.00 & 0.00 \\ & & & 5.33 & 0.00 & 0.00 \\ & & & & 4.98 & 0.00 \\ & & & & & 4.98 \end{pmatrix}$$

and

$$
\begin{pmatrix}
20.42 & 6.80 & 6.80 & 0.00 & 0.00 & 0.00 \\
 & 23.96 & 7.69 & 0.00 & 0.00 & 0.00 \\
 & & 23.96 & 0.00 & 0.00 & 0.00 \\
 & & & 8.13 & 0.00 & 0.00 \\
 & & & & 7.60 & 0.00 \\
 & & & & & 7.60
\end{pmatrix}.
$$

The elastic parameters between the depths of 0.0 and 1.0 km are determined again by linear interpolation. The density is constant and equals 1.0 g/cm^3. Sections of the qS wave phase velocity surfaces by the plane of experiment at the depths of 0.0 and 0.6 km are shown in Fig.4.

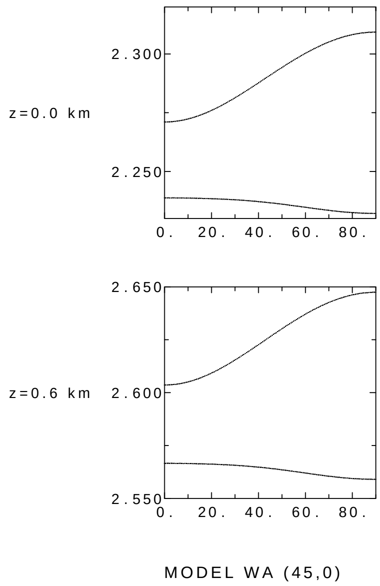

Figure 4

Anisotropy in these sections is stronger than in the model EWA, it varies from 1% for horizontal propagation to 4% for vertical propagation.

Calculation of qS wave field for EWA model

Figures 5 to 7 show in the left column from the bottom to the top ray diagrams (projections into the plane of experiment and into the horizontal plane) and travel times. In the right column, decadic logarithms of ray amplitudes corresponding to the considered vertical force source are shown. Figure 5 shows an S wave in an isotropic (ISO) background model whose parameters are following: P and S waves velocities at $z = 0.0km$ are 4.5 and 2.53 km/s. For the depth of 1.0 km, they are 5.56 and 3.12 km/s. The density is constant and equal to 1.0 g/cm^3. We can see that rays to all receivers were found and that these rays are confined within the plane of experiment. Let us emphasize that the generated S wave has a pure SV polarization, its transverse component being zero.

Figures 6 and 7 show $qS1$ and $qS2$ waves calculated using the ray method for inhomogeneous anisotropic media. We can see that in this case the rays do not illuminate

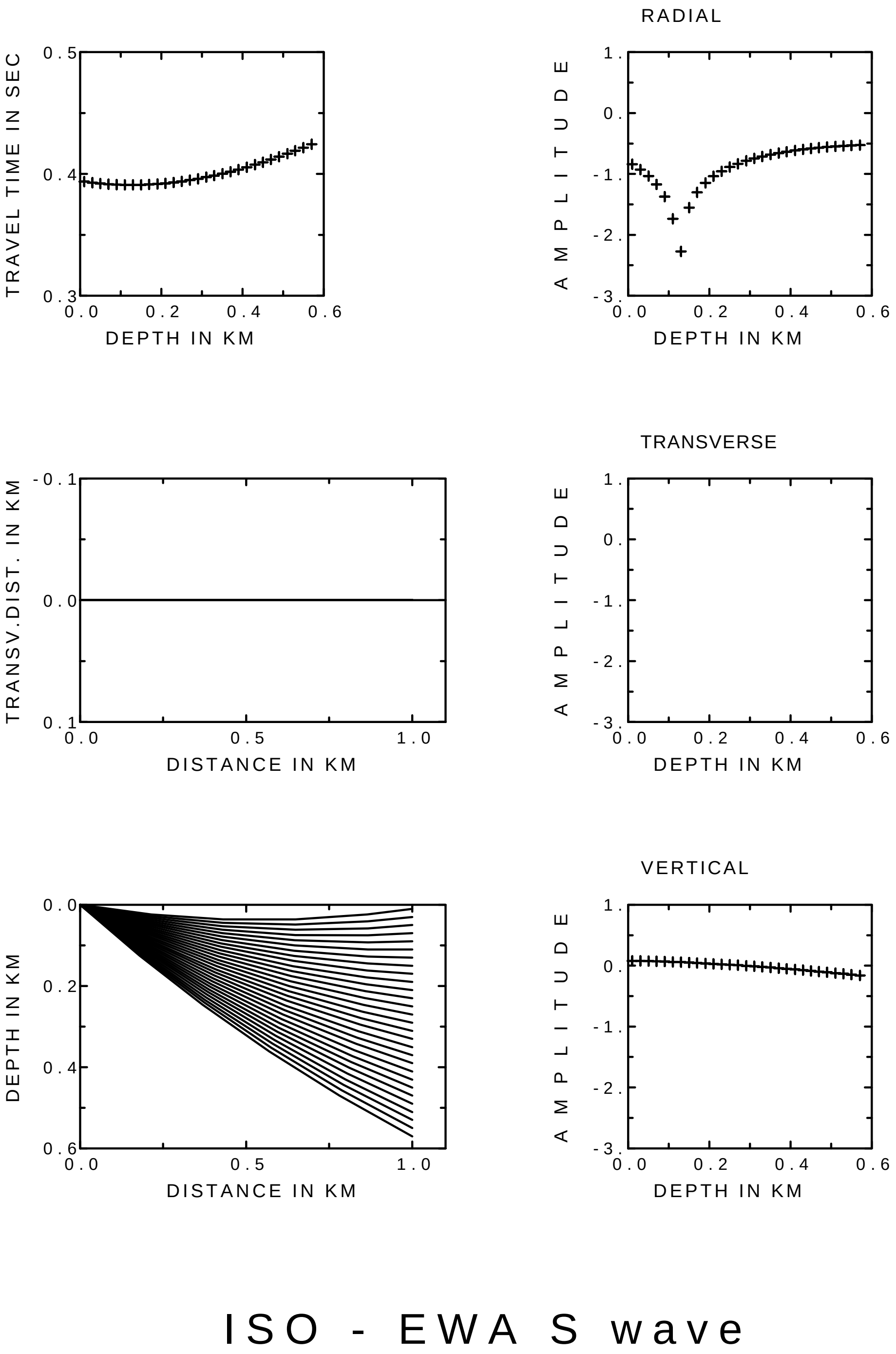

Figure 5

all the receivers. The reason is breakdown of the ray code due to the shear wave singularity shown in Fig.3. The deviation of rays, which are successfully calculated, from the plane of experiment is negligible, see the projections into the horizontal plane. Both ray diagrams in Figs. 6 and 7 as well as the travel time curves are nearly identical to the

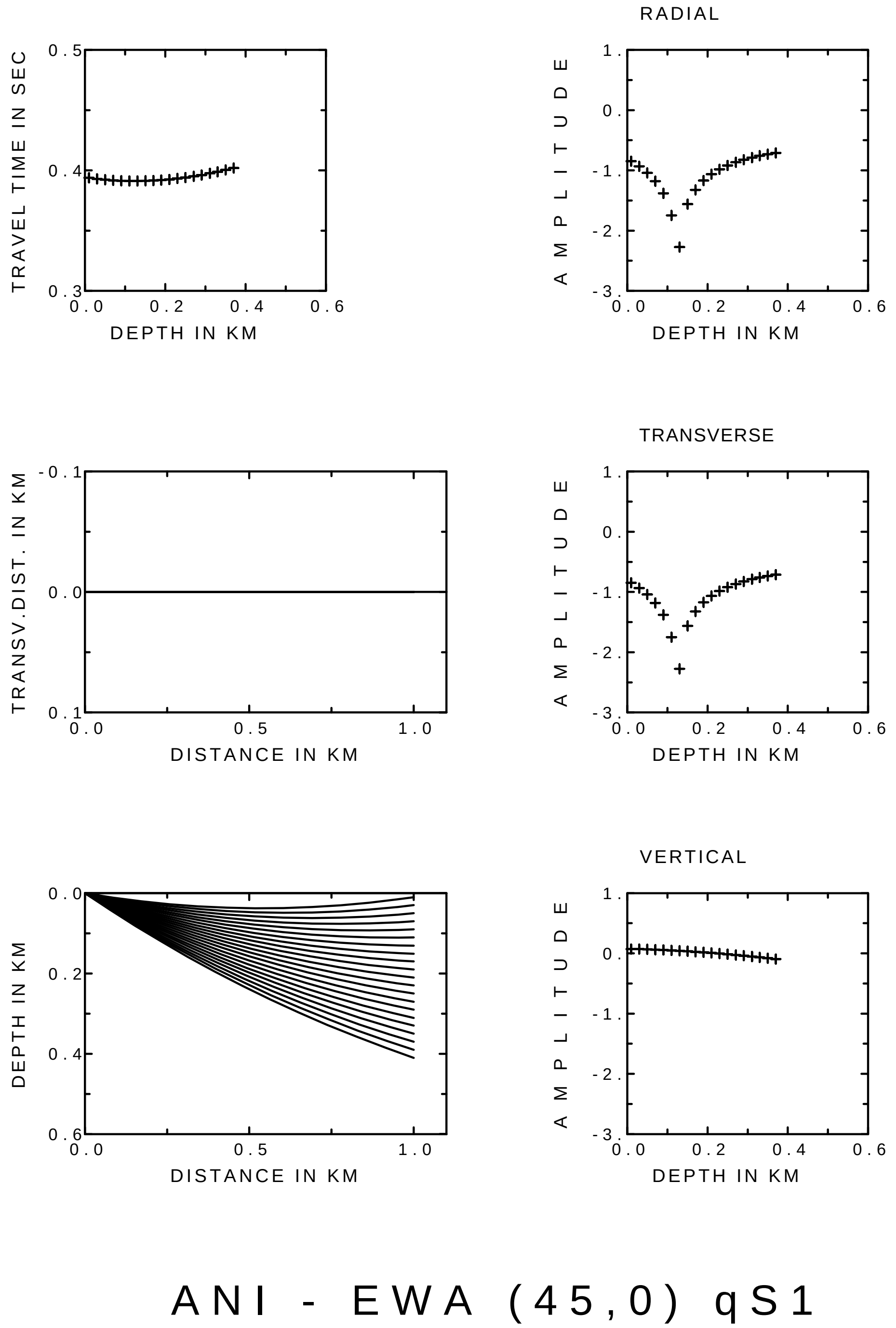

Figure 6

corresponding parts of the ray diagram and the travel time curve in Fig.5. This is because of closeness of the considered anisotropic medium to an isotropic one. There is, however, a remarkable difference in behaviour of ray amplitudes. None of the two qS waves is polarized purely SV or SH. The $qS1$ wave (the faster wave) has polarization closer to

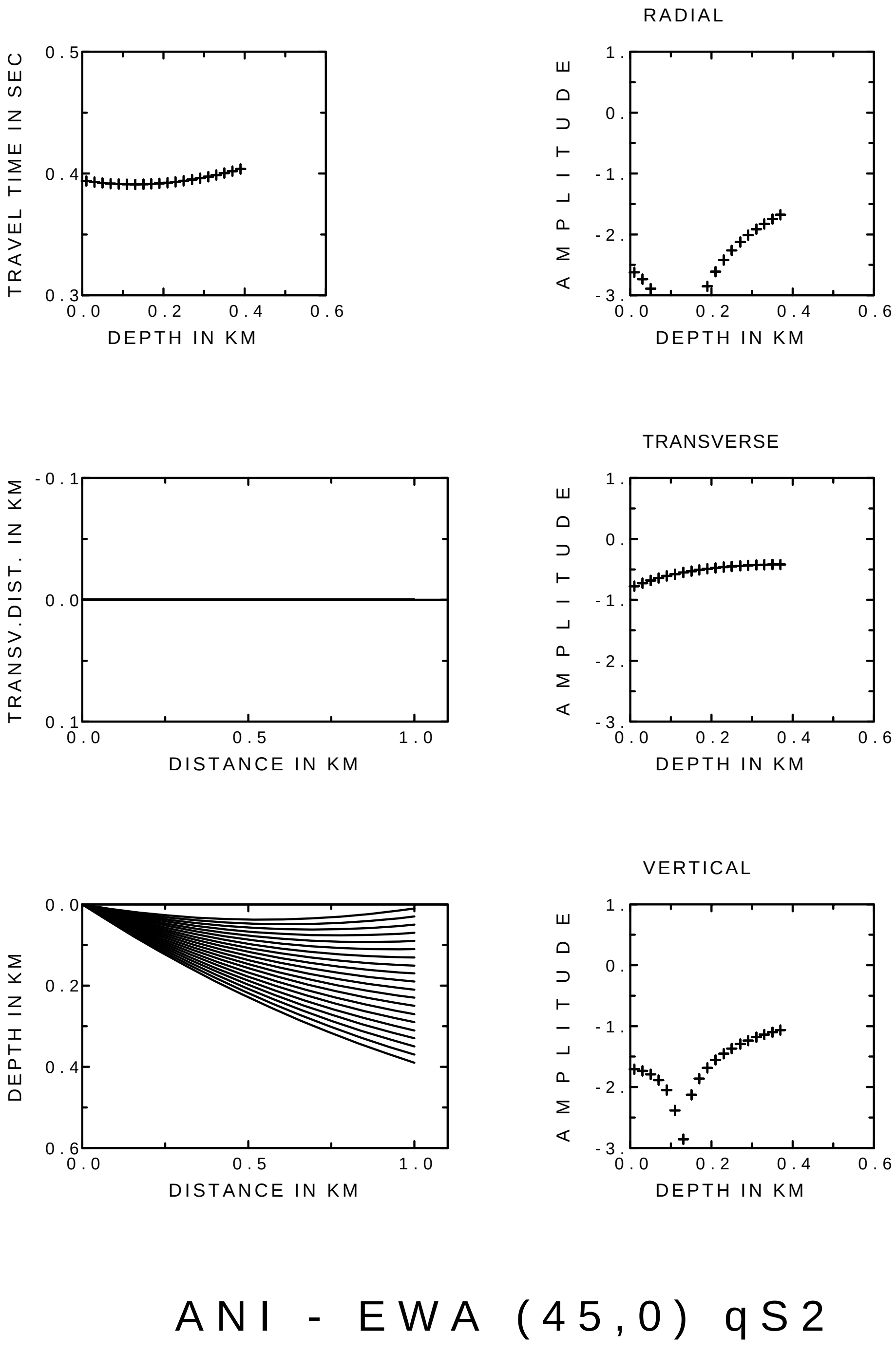

Figure 7

SV, the $qS2$ wave closer to SH. In a medium, which is nearly isotropic, a vertical force should generate only SV polarized shear wave as in Fig.5. Thus the ray method for anisotropic media gives distorted results in Figs.6 and 7.

Figures 8 to 10 show synthetic seismograms of qS waves calculated for the configuration specified above. Prevailing frequency of the source-time function shown in Fig.2 is 50 Hz. In Fig.8, we can see that although the medium is practically isotropic and the source generating waves is a vertical force, standard ray method for anisotropic media yields a wave with rather strong transverse component. The transverse component is, in fact, stronger than the radial one. We can again see that the deeper receivers are not illuminated because of the breakdown of the ray tracer. On the radial component we can observe the change of polarization (see also Figs.9 and 10) caused by arrival of rays to the shallow receivers from below and to the deeper rays from above.

Figure 9 shows seismograms calculated for the background isotropic medium. We can see that the wave field is correctly confined to the plane of experiment only (zero transverse component).

Figure 10 is a result of the QI approach. We can see that the whole picture very closely resembles the picture in Fig.9, i.e. the picture for isotropic medium. There are some disturbances on the transverse component but they are negligible when compared with remaining components. Note the values of scaling factors (the last number of four numbers over the upper right corner of each seismogram plot). They are very close to the numbers in Fig.9 but differ from scaling factors of ANI seismograms.

Even more illustrative is to compare particle motion diagrams calculated for selected receivers with the ray method for isotropic media, with the QI approach and with the ray method for anisotropic media. The calculations for the background isotropic medium can serve as a reference and we present them now, therefore, first. We select three receivers at depth of z=0.01, 0.29 and 0.57 km. They thus represent shallow, intermediate and deep receivers. Results are shown in Figs.11-13.

Figure 11 shows particle motion diagrams for the isotropic model. Polarization is strictly linear. The pictures on the bottom line indicate that the wave arrives to the shallow receiver from below, to the other receivers from above. We can see that the polarization of the wave is purely SV.

Figure 12 shows results of the QI approach. Only little deviations from Fig.11 can be observed. In contrast to Fig.11, the particle motion displays a weak quasi-ellipticity. The polarization is, however, again prevailingly SV.

Figure 13 differs from the previous figures in two main aspects. First, due to the above mentioned breakdown of the ray method for anisotropic media, there are no observations at the deepest receiver. Second, Fig.13 clearly shows that the calculated wave has quite significant SH component. This is in contradiction with the used nearly isotropic model and vertical force source.

The above comparison shows that the QI approach models very well the qS wave field both in a region of weak anisotropy and in a region of intersection singularity.

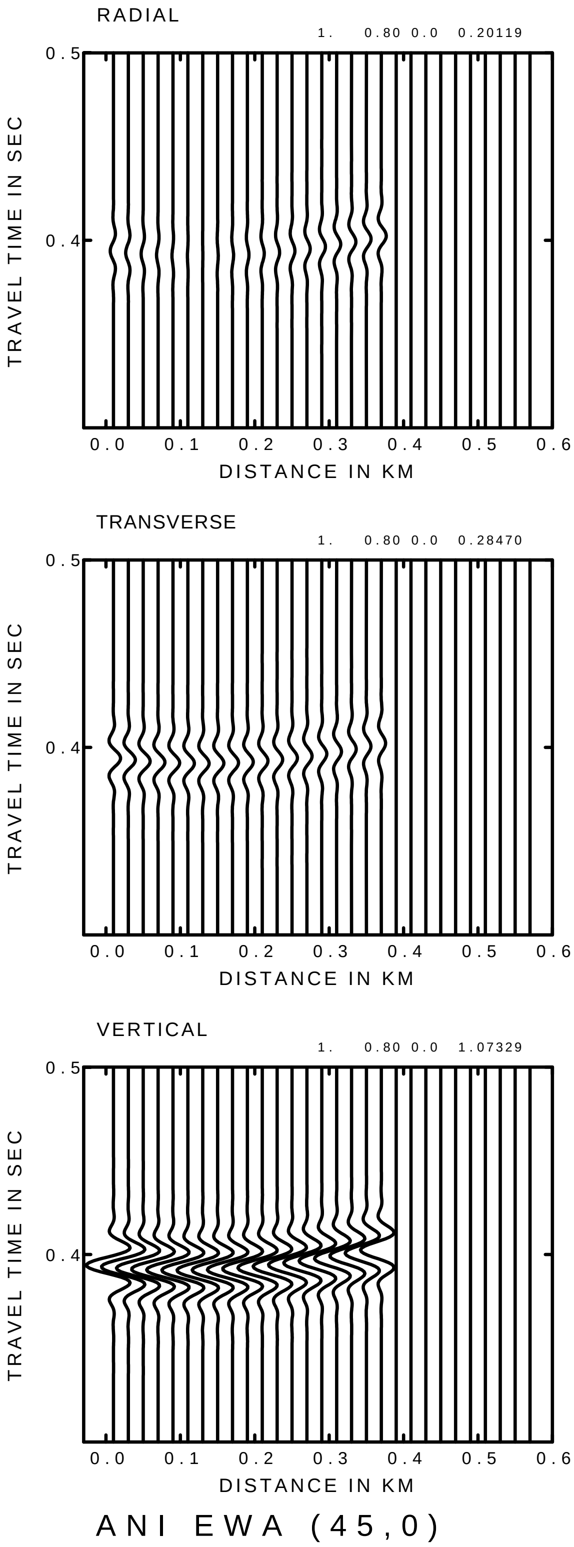

RADIAL
1. 0.80 0.0 0.20119
0.5
0.4
TRAVEL TIME IN SEC
0.0 0.1 0.2 0.3 0.4 0.5 0.6
DISTANCE IN KM
TRANSVERSE
1. 0.80 0.0 0.28470
0.5
0.4
TRAVEL TIME IN SEC
0.0 0.1 0.2 0.3 0.4 0.5 0.6
DISTANCE IN KM
VERTICAL
1. 0.80 0.0 1.07329
0.5
0.4
TRAVEL TIME IN SEC
0.0 0.1 0.2 0.3 0.4 0.5 0.6
DISTANCE IN KM
ANI EWA (45,0)

Figure 8

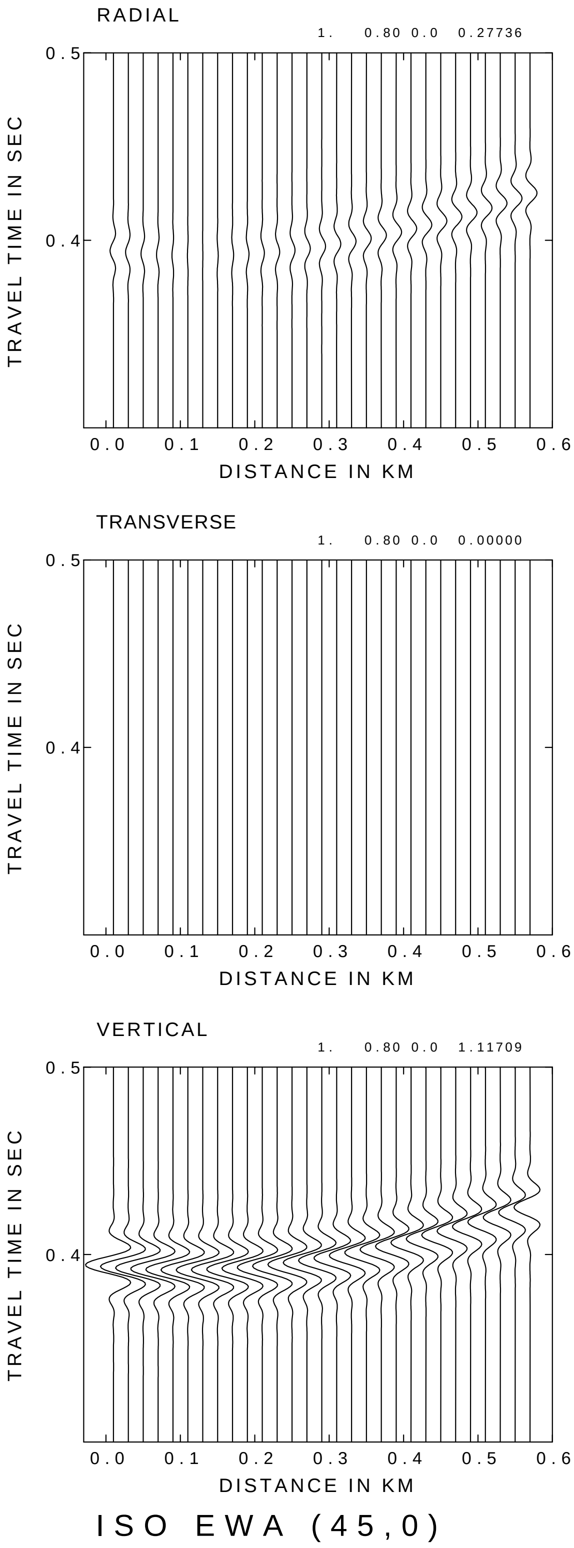
RADIAL
1. 0.80 0.0 0.27736
TRAVEL TIME IN SEC
0.5
0.4
0.0 0.1 0.2 0.3 0.4 0.5 0.6
DISTANCE IN KM
TRANSVERSE
1. 0.80 0.0 0.00000
TRAVEL TIME IN SEC
0.5
0.4
0.0 0.1 0.2 0.3 0.4 0.5 0.6
DISTANCE IN KM
VERTICAL
1. 0.80 0.0 1.11709
TRAVEL TIME IN SEC
0.5
0.4
0.0 0.1 0.2 0.3 0.4 0.5 0.6
DISTANCE IN KM
ISO EWA (45,0)

Figure 9

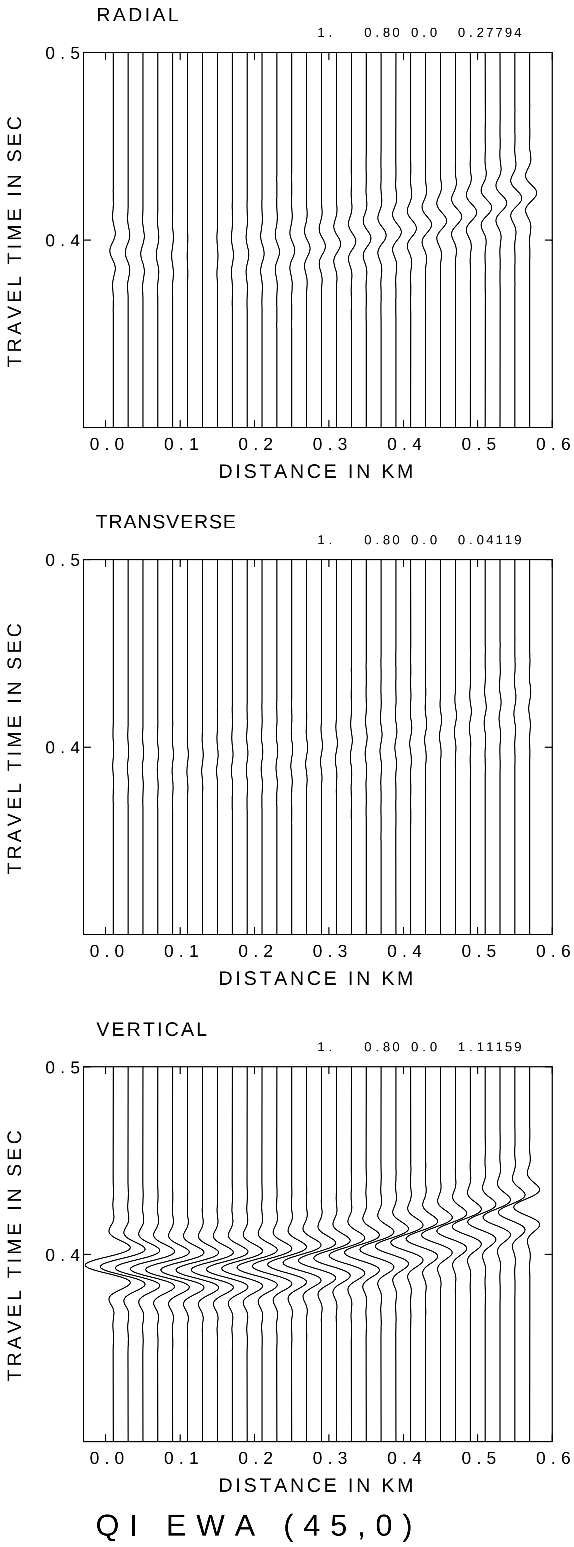

RADIAL
1. 0.80 0.0 0.27794
TRAVEL TIME IN SEC
0.5
0.4
0.0 0.1 0.2 0.3 0.4 0.5 0.6
DISTANCE IN KM
TRANSVERSE
1. 0.80 0.0 0.04119
TRAVEL TIME IN SEC
0.5
0.4
0.0 0.1 0.2 0.3 0.4 0.5 0.6
DISTANCE IN KM
VERTICAL
1. 0.80 0.0 1.11159
TRAVEL TIME IN SEC
0.5
0.4
0.0 0.1 0.2 0.3 0.4 0.5 0.6
DISTANCE IN KM
QI EWA (45,0)

Figure 10

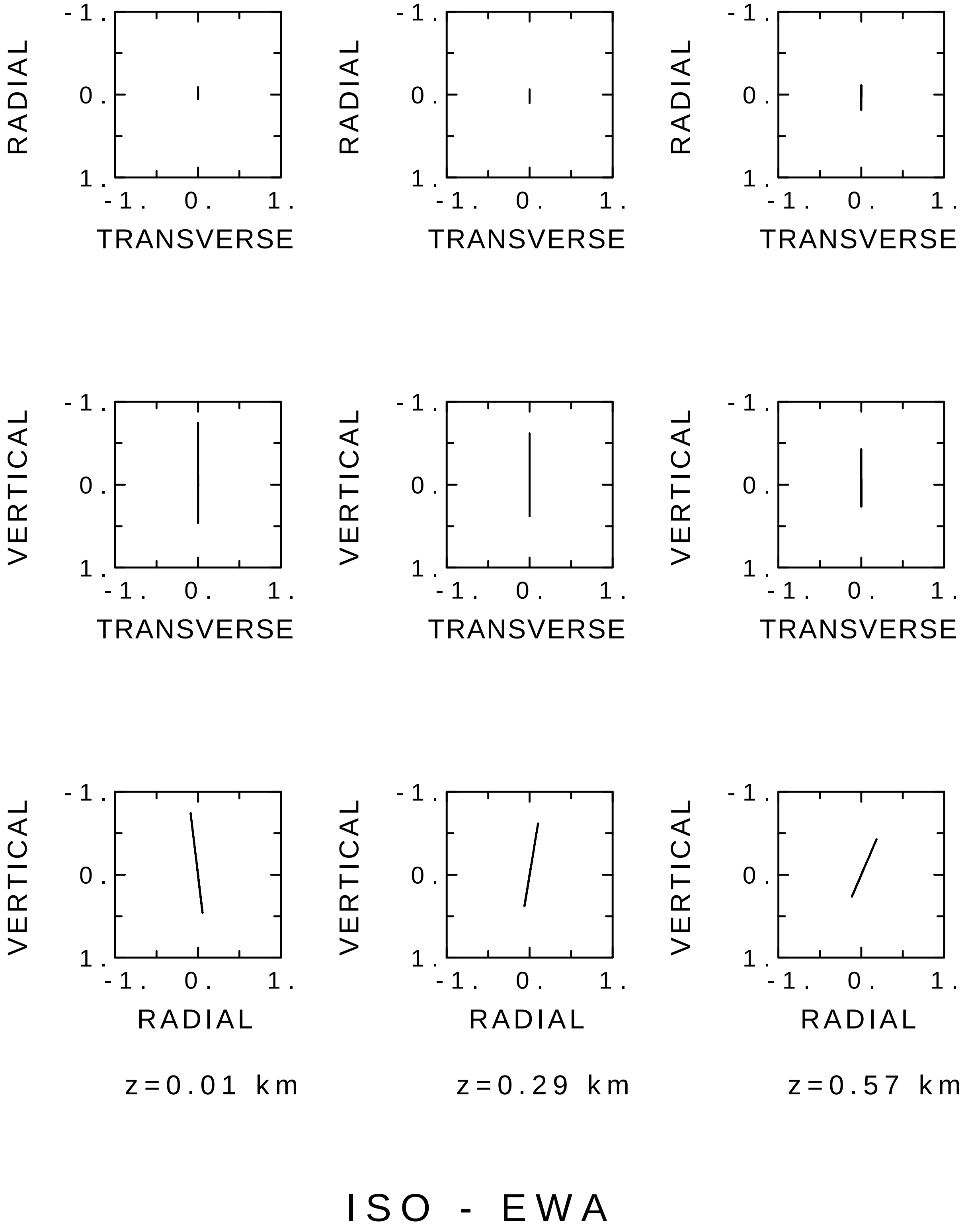
RADIAL
TRANSVERSE
VERTICAL
RADIAL
-1.
0.
1.
z=0.01 km
z=0.29 km
z=0.57 km
ISO - EWA

Figure 11

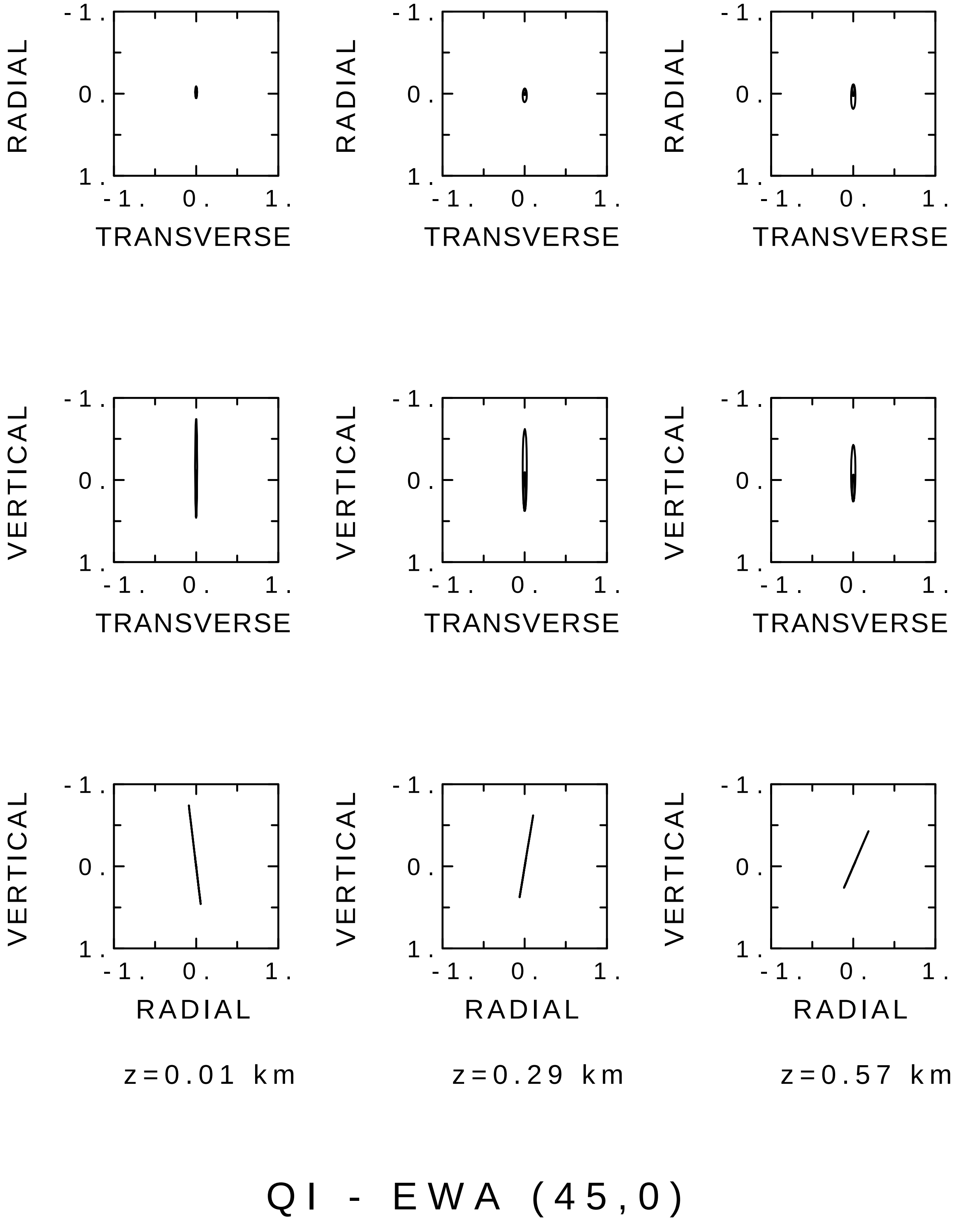
RADIAL
TRANSVERSE
VERTICAL
-1.
0.
1.
z=0.01 km
z=0.29 km
z=0.57 km
QI - EWA (45,0)

Figure 12

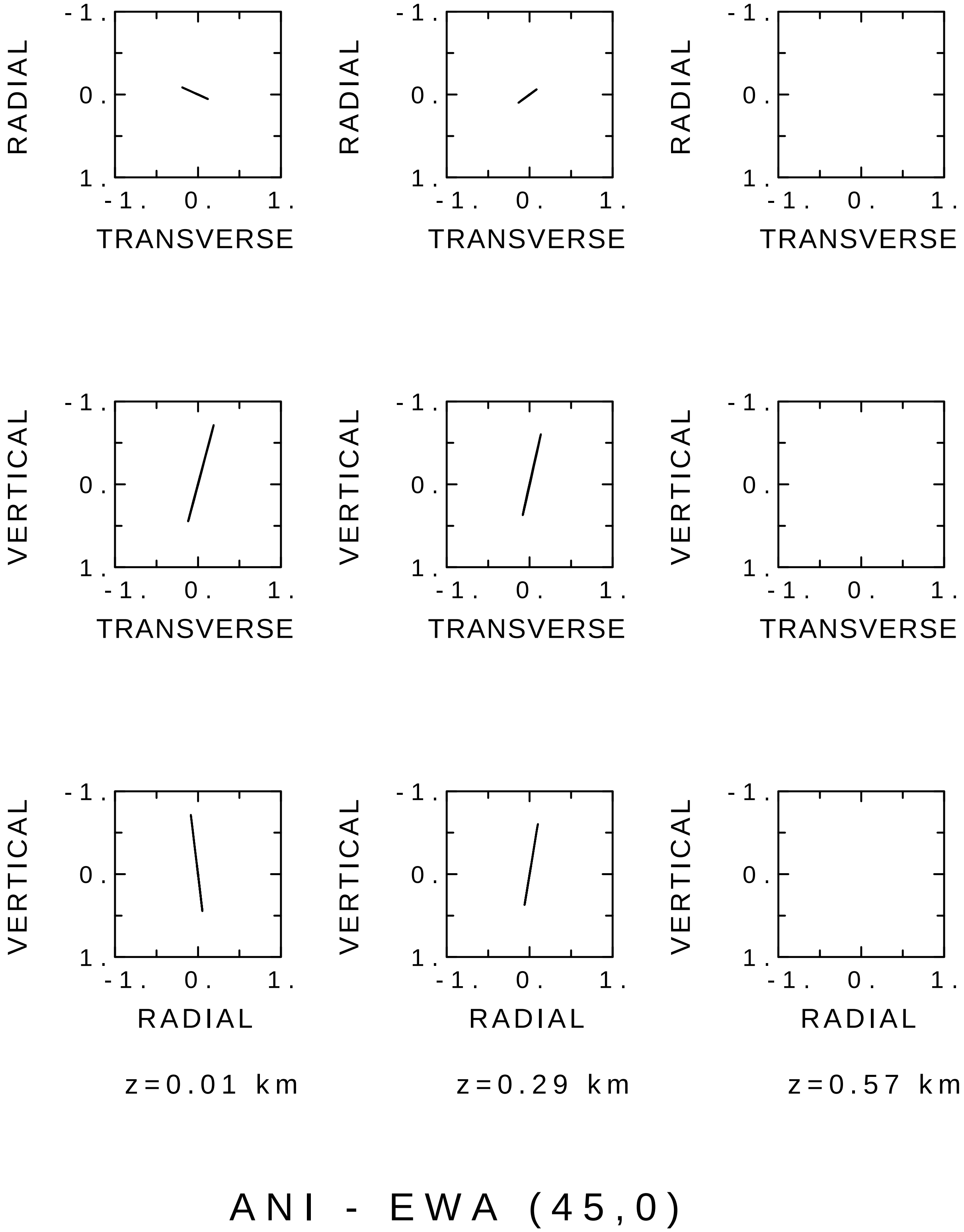

-1.
0.
1.
RADIAL
TRANSVERSE
VERTICAL
z=0.01 km
z=0.29 km
z=0.57 km
ANI - EWA (45,0)

Figure 13

Calculation of qS wave field for WA model

Figures 14 to 16 show again ray diagrams and travel time and amplitude distance curves generated by the vertical force source. Fig. 14 shows an S wave in an isotropic (ISO)

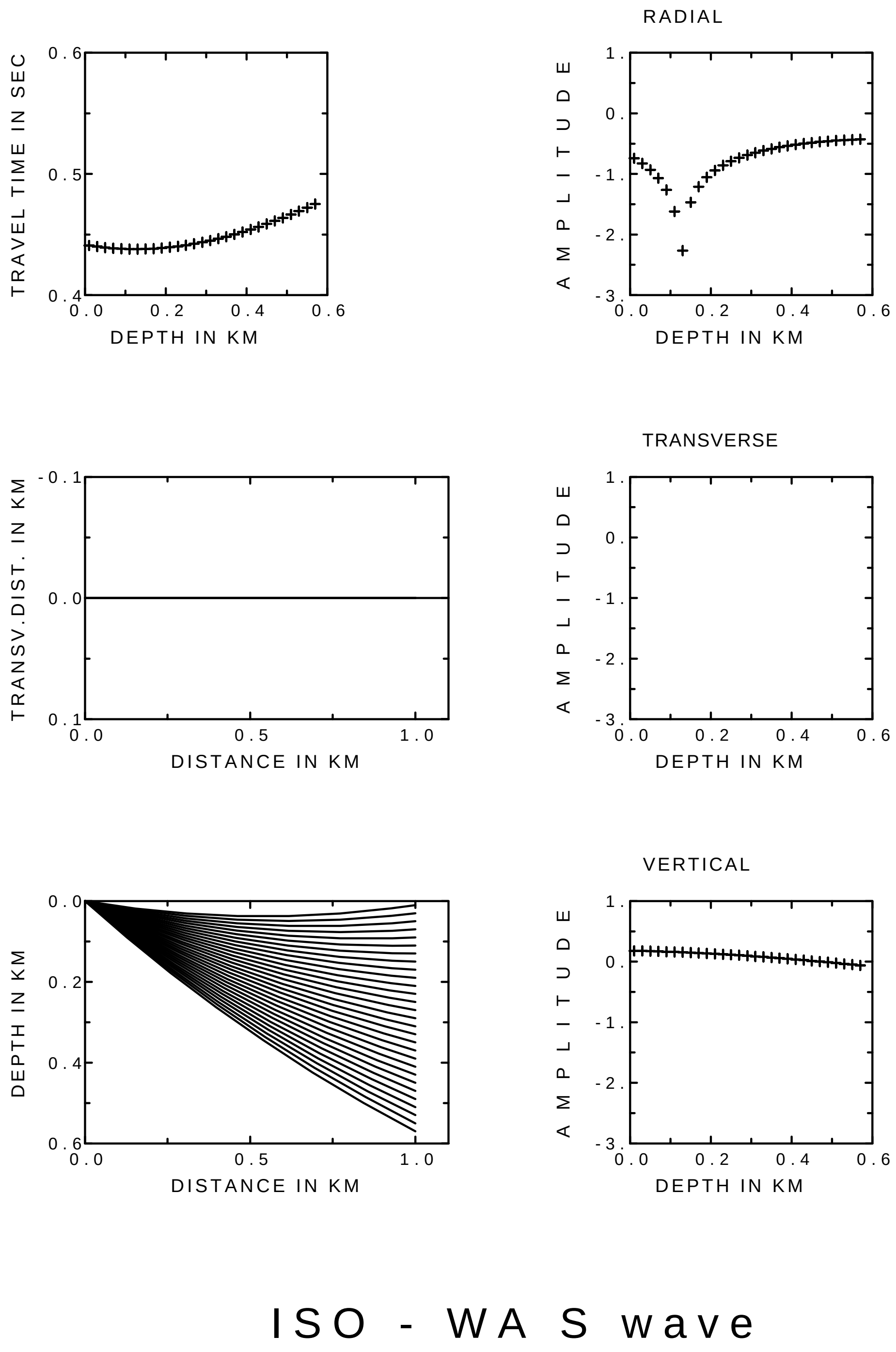

Figure 14

background model with following parameters: P and S wave velocities at $z = 0.0$ km are 3.87 and 2.26 km/s, at $z = 1.0$ km, they are 4.8 and 2.79 km/s. The density is constant and equal to 1.0 g/cm^3. The generated S wave is purely SV polarized.

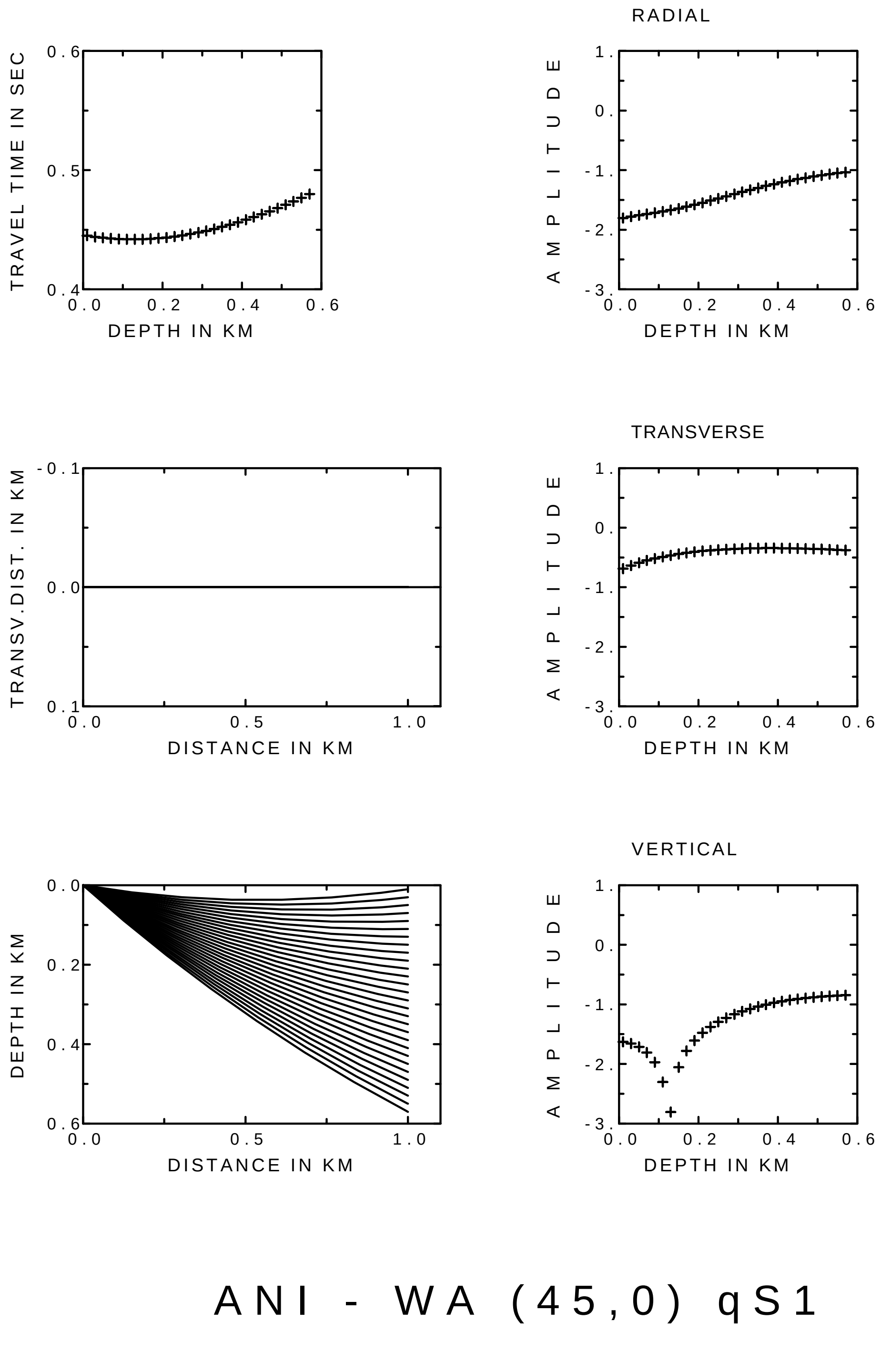

Figure 15

Figures 15 and 16 show $qS1$ and $qS2$ waves calculated using the ray method for inhomogeneous anisotropic media.We can see that now we found rays to all receivers and that these rays are confined within the plane of experiment.

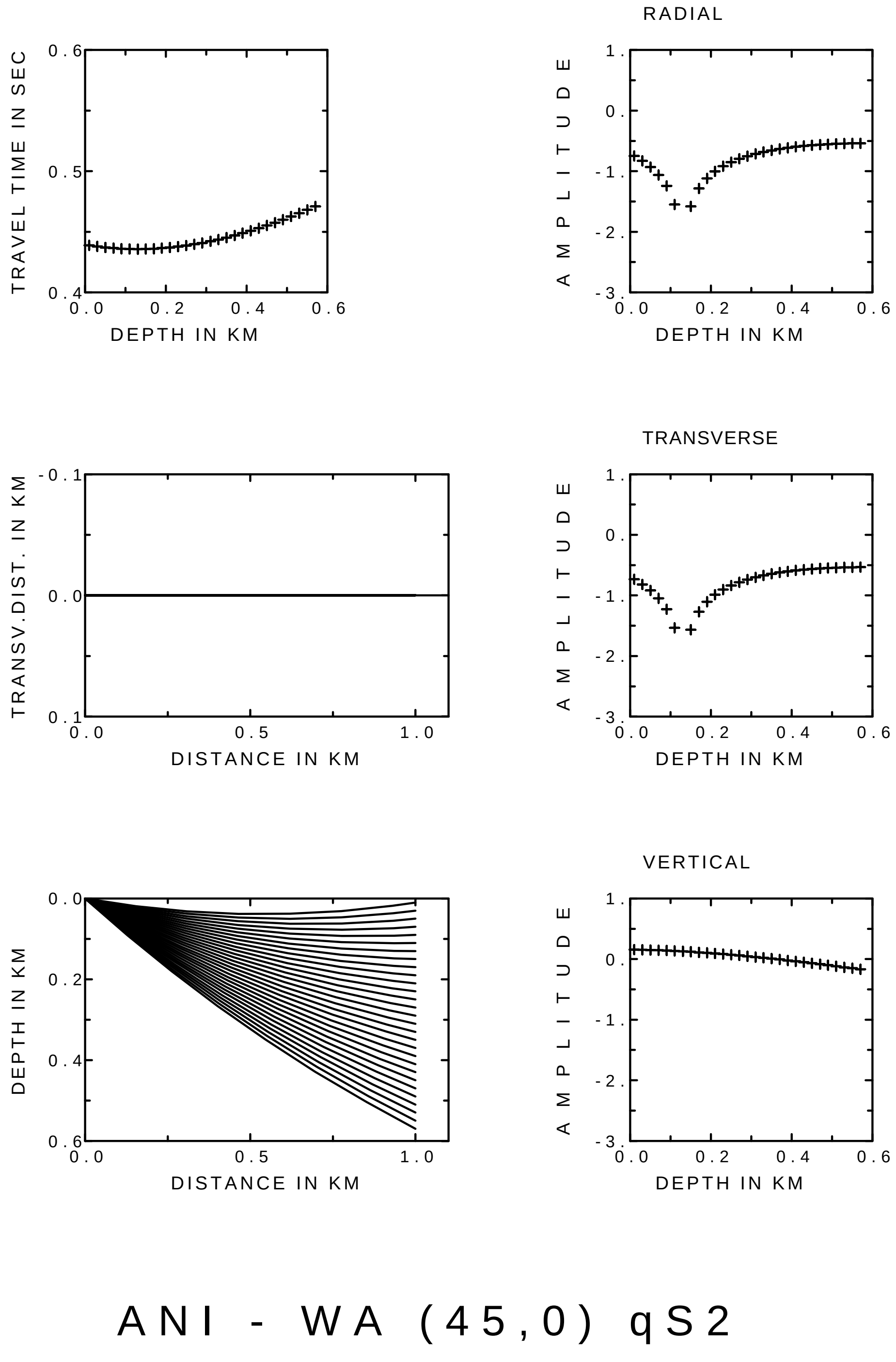

Figure 16

Since anisotropy of the model is stronger than in the EWA model, there are observable differences in the travel times of $qS1$ and $qS2$ waves. We can see that none of these waves is polarized purely SV. SV polarization prevails now for slower $qS2$ wave, SH polarization prevails for $qS1$ wave.

Figures 17 to 19 show synthetic seismograms of qS waves calculated again for the configuration specified above. Prevailing frequency of the source-time function is 50 Hz. In Fig.17 we can see seismograms calculated by the ray method for anisotropic media. In Fig.18 seismograms calculated by the ray method for isotropic media for the model of the background isotropic medium. Finally, in Fig.19, we can see the results of the QI approach. In this case, we can see that the QI results, although different in details, resemble more the results of the ray method for anisotropic media (Fig.17) than the ray method for isotropic media (Fig.18), compare also the scaling factors. This is because of stronger anisotropy and high prevailing frequency of the considered source-time signal. We can see that the QI approach generates waves with a rather strong transverse component in this case. In order to detect greater details, let us check the particle motion diagrams constructed for the same three receivers as above, i.e., for depth of z=0.01, 0.29 and 0.57 km. Results are shown in Figs.20-22.

Figure 20 shows particle motion diagrams for the isotropic model. It has the same features as the particle motion diagrams in Fig.11. It shows pure SV polarization of the observed S wave.

Figure 21, which shows the particle motion diagrams calculated by the QI approach, differs substantially from Fig.20 for the intermediate and deep receivers. The particle motion is nonlinear and the polarization is a mixture of the SV and SH polarization. The particle motion for the shallow receiver, however, differs only slightly from its "isotropic" counterpart.

Figure 22, obtained with the ray method for anisotropic media yields for the intermediate and deep receivers results, which closely resemble results obtained with the QI approach. The diagrams for the shallow receiver differ by a greater nonlinearity of the results of the ray method for anisotropic media and indications of slight transverse components.

We thus obtained an interesting result in Fig.21. For the shallow receiver the QI approach converges to the "isotropic" results while for the deeper receivers it converges to the "anisotropic" results. It is because for the shallow receivers the difference between two qS wave phase velocities is smaller than for deeper receivers, see Fig.4, and also the waves travel a shorter distance from the source to a receiver. The qS waves propagate to shalow receivers through a medium, which resembles more isotropic than anisotropic medium. For deeper receivers the difference in qS wave phase velocities is larger and the waves travel larger distances so that they can decouple and separate, see the differences in travel times in Figs.15 and 16. Quite pronounced quasi-elliptical polarization in Figs.21 and 22 is a consequence of this separation - shear wave splitting. While the quasi-elliptical polarization in Fig.22 results naturally from the interference of two qS waves calculated along different ray paths shown in Figs.15 and 16, in Fig.21 its origin is not so straightforward. The quasi-elliptical polarization in Fig.21 is a result of solution of two coupled differential

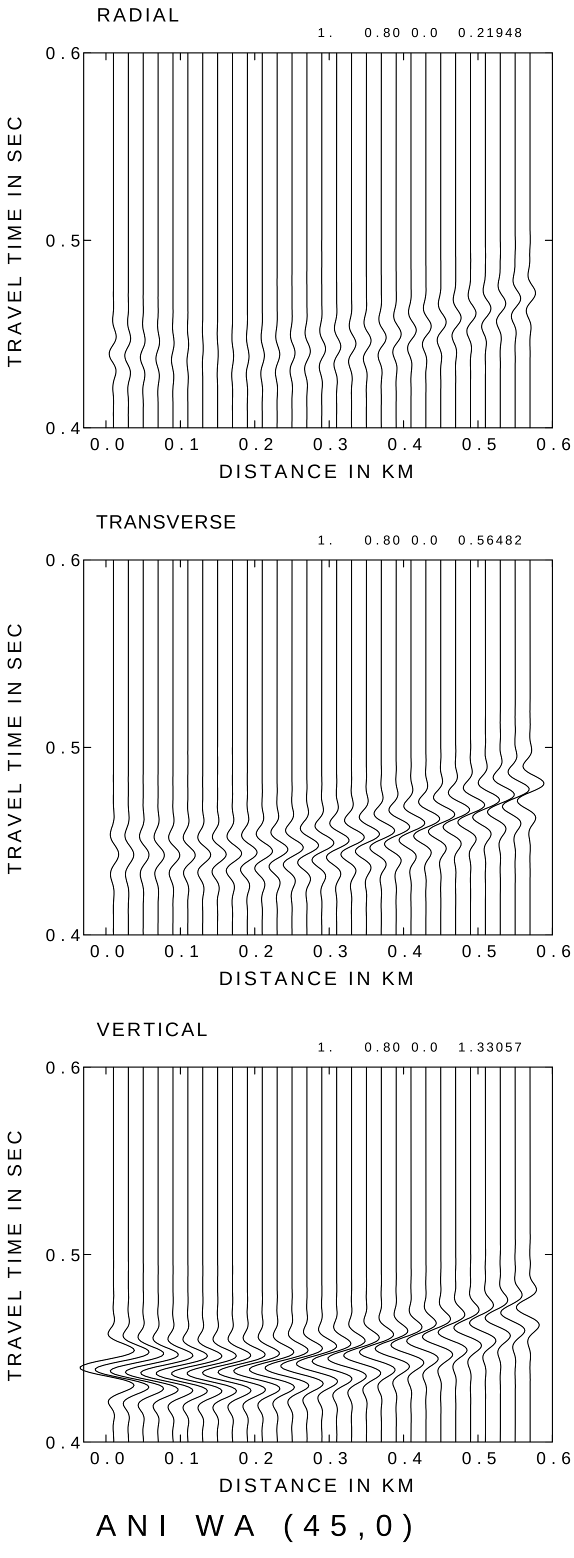
RADIAL
1. 0.80 0.0 0.21948
TRAVEL TIME IN SEC
DISTANCE IN KM
TRANSVERSE
1. 0.80 0.0 0.56482
TRAVEL TIME IN SEC
DISTANCE IN KM
VERTICAL
1. 0.80 0.0 1.33057
TRAVEL TIME IN SEC
DISTANCE IN KM
ANI WA (45,0)

Figure 17

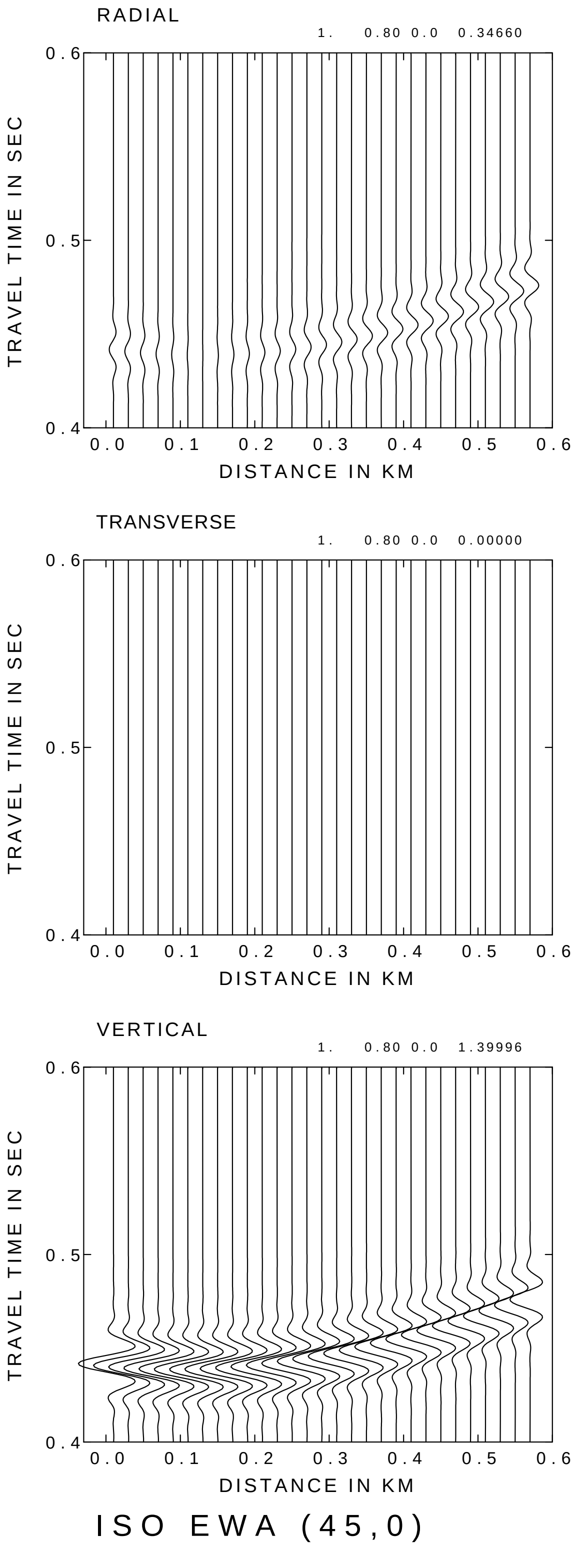
RADIAL
1. 0.80 0.0 0.34660
TRAVEL TIME IN SEC
DISTANCE IN KM
TRANSVERSE
1. 0.80 0.0 0.00000
TRAVEL TIME IN SEC
DISTANCE IN KM
VERTICAL
1. 0.80 0.0 1.39996
TRAVEL TIME IN SEC
DISTANCE IN KM
ISO EWA (45,0)

Figure 18

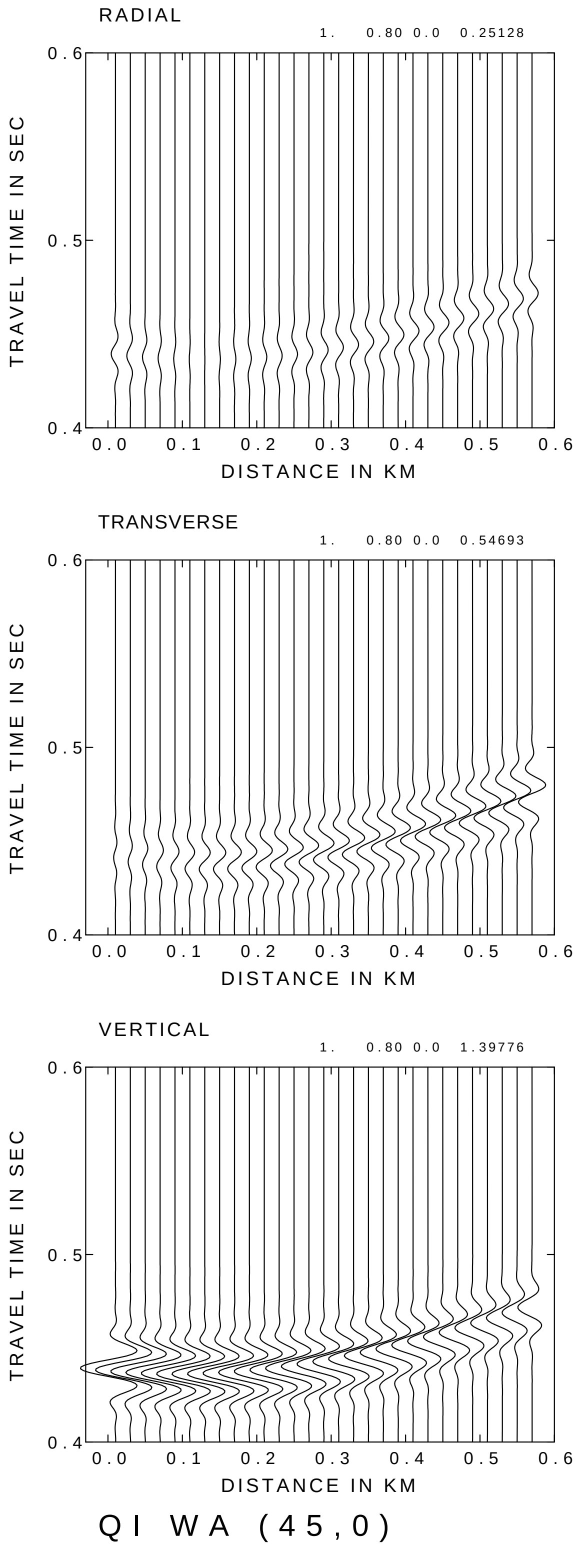

RADIAL
1. 0.80 0.0 0.25128
TRAVEL TIME IN SEC
0.6
0.5
0.4
0.0 0.1 0.2 0.3 0.4 0.5 0.6
DISTANCE IN KM
TRANSVERSE
1. 0.80 0.0 0.54693
TRAVEL TIME IN SEC
0.6
0.5
0.4
0.0 0.1 0.2 0.3 0.4 0.5 0.6
DISTANCE IN KM
VERTICAL
1. 0.80 0.0 1.39776
TRAVEL TIME IN SEC
0.6
0.5
0.4
0.0 0.1 0.2 0.3 0.4 0.5 0.6
DISTANCE IN KM
QI WA (45,0)

Figure 19

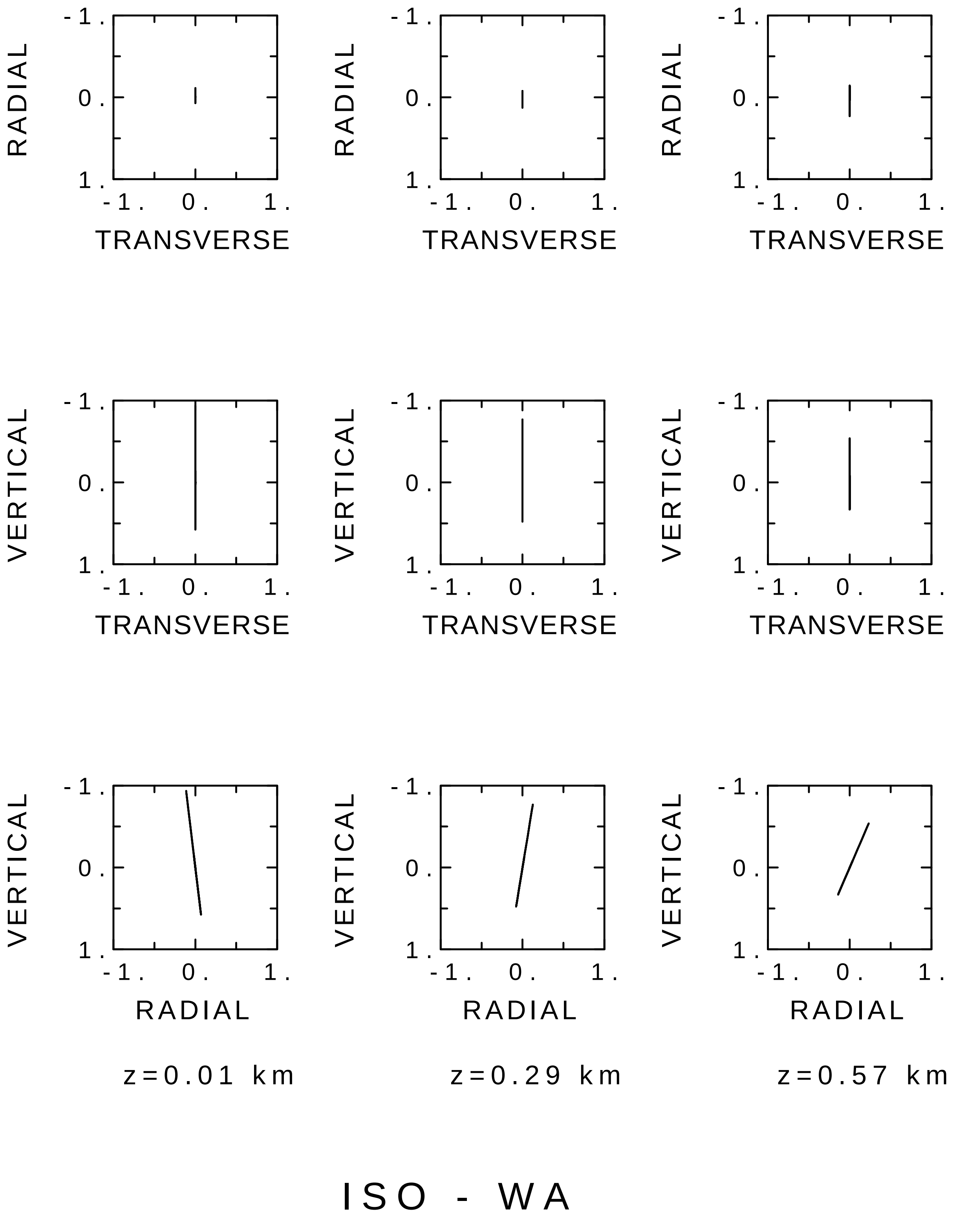

-1.
0.
1.
RADIAL
TRANSVERSE
VERTICAL
z=0.01 km
z=0.29 km
z=0.57 km
ISO - WA

Figure 20

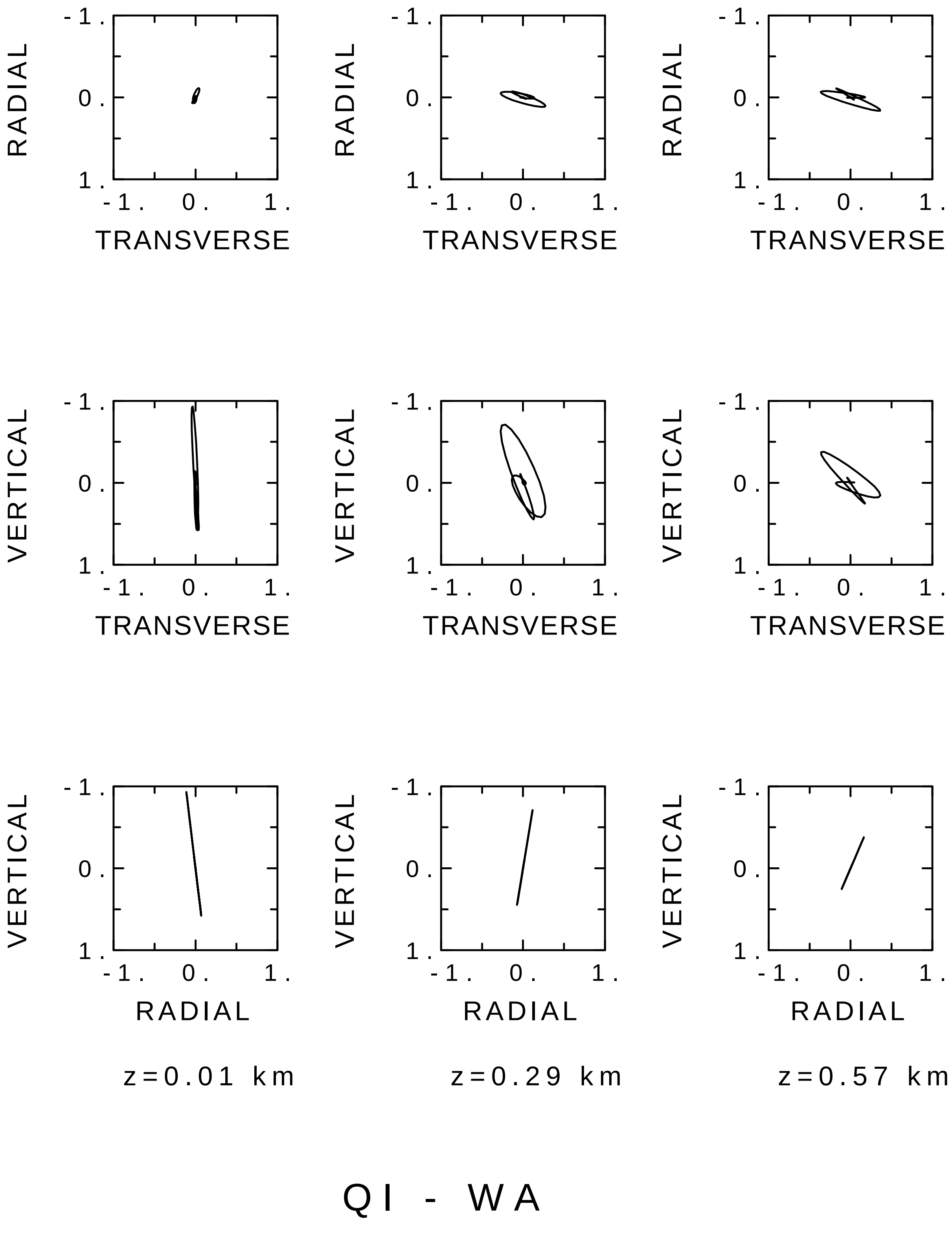
RADIAL
TRANSVERSE
VERTICAL
RADIAL
-1.
0.
1.
z=0.01 km
z=0.29 km
z=0.57 km
QI - WA

Figure 21

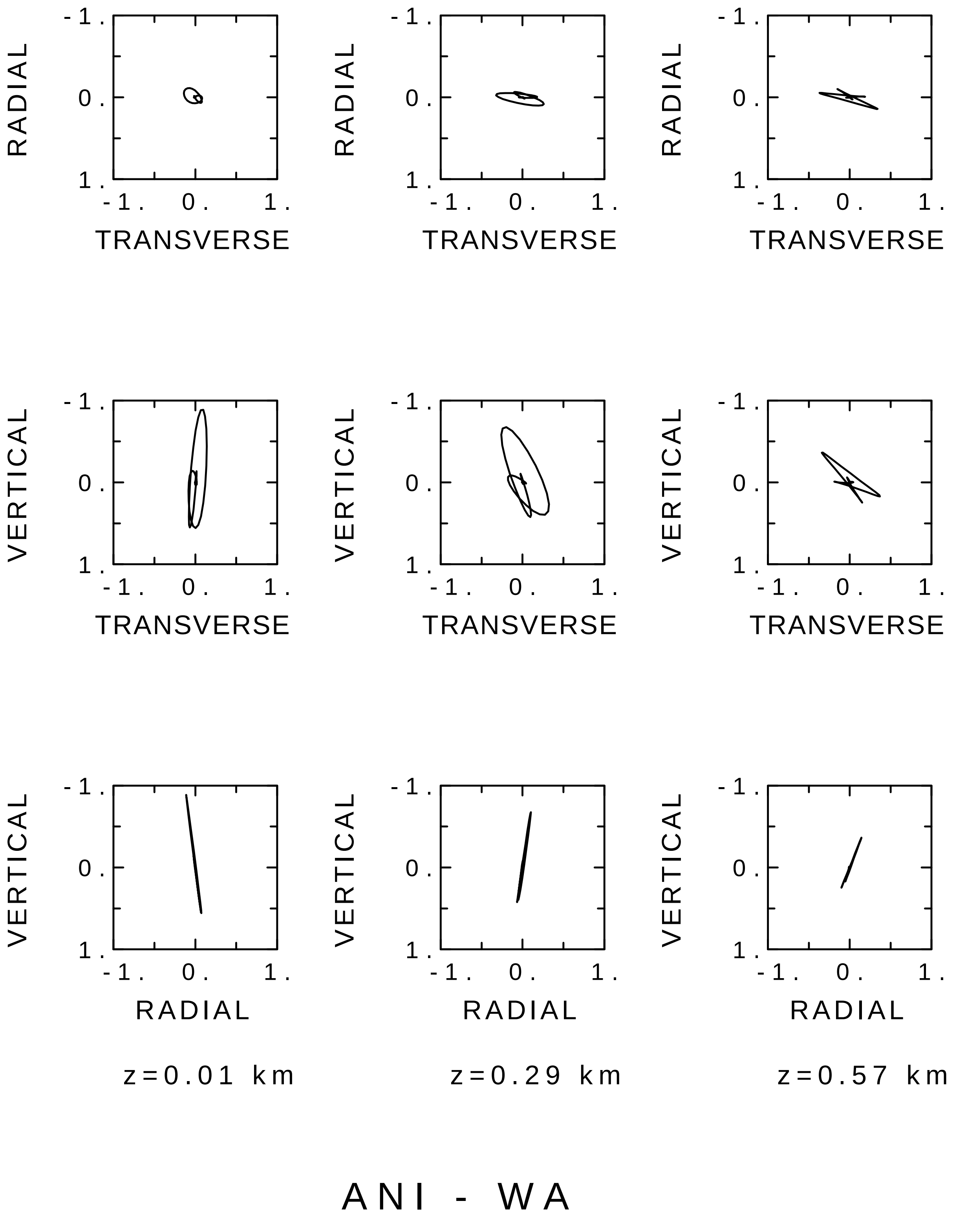

RADIAL
TRANSVERSE
VERTICAL
-1.
0.
1.
z=0.01 km
z=0.29 km
z=0.57 km
ANI - WA

Figure 22

eqautions for the QI amplitudes calculated along a single ray of an S wave in the background isotropic medium. If extrapolation of the qS wave field behind the intermediate and deep receivers were required, the QI approach could be, in principle, substituted by the standard ray method for anisotropic media. From the region of these receivers, two qS waves could be calculated along two different ray paths.

Let us now study effects of prevailing frequency of the source signal on the results of the QI approach. We first decrease the prevailing frequency to 25 Hz. Figures 23 - 25 show corresponding synthetic seismograms in the same order as above. For shallow receivers the QI seismograms (Fig.25) resemble now seismograms calculated by the ray method for isotropic media (Fig.24), for deeper receivers they resemble more seismograms calculated by the ray method for anisotropic media (Fig.23). If we compare the transverse component in Fig.25 with the same component calculated by the QI approach for 50 Hz in Fig.19, we can see a substantial difference, see also the scaling factors. The transverse component at shallow receivers for prevailing frequency of 25 Hz is very weak, which means that the wave at these receivers is polarized prevailingly SV. This can be seen more clearly on particle motion diagrams in Figs.26 -28. Particle motions calculated for the background isotropic model (Fig.26) are practically identical with the particle motions for frequency 50 Hz shown in Fig.20. Particle motions calculated by the QI approximation (Fig.27) differ now more from the particle motions calculated by the ray method for anisotropic media (Fig.28). The particle motion for the shallowest receiver is now nearly identical with the "isotropic" particle motion. It is purely linearly polarized. The particle motions at intermediate receiver also seems to "converge" to "isotropic" particle motion. This trend continues even further if frequency of 10 Hz is considered. The results are shown in Figs.29 - 34. In seismograms calculated by the QI approach (Fig.31), we can see an overall reduction of the transverse component, For shallow receivers, the transverse component is effectively zero. The effect of convergency of the QI results to the results obtained by the ray method for isotropic media can be seen even clearer in particle motion diagrams. Although the polarization at intermediate and deep receivers is still nonlinear, it becomes more confined to the plane of experiment, compare transverse - vertical and transverse - radial diagrams in Figs.32 and 33. Further decrease of frequency would lead to coincidence of the QI results with "isotropic" ones.

CONCLUSIONS

First results obtained by the zero-order approximation of the QI approach for qS waves in inhomogeneous weakly anisotropic media were presented. The results confirm conclusions of theoretical studies, according to which the QI approach represents a link between the ray methods for isotropic and anisotropic media. On a model with extremaly weak anisotropy, the QI approximation gave results, which coincide with results of the ray method for isotropic media. When anisotropy was stronger and frequency of studied waves high, the QI approximation gave results, which coincided with results of the ray method for anisotropic media. Thus the QI approach does not only fill the gap between both ray methods but the regions of its applicability seem to overlap regions of applicability of the

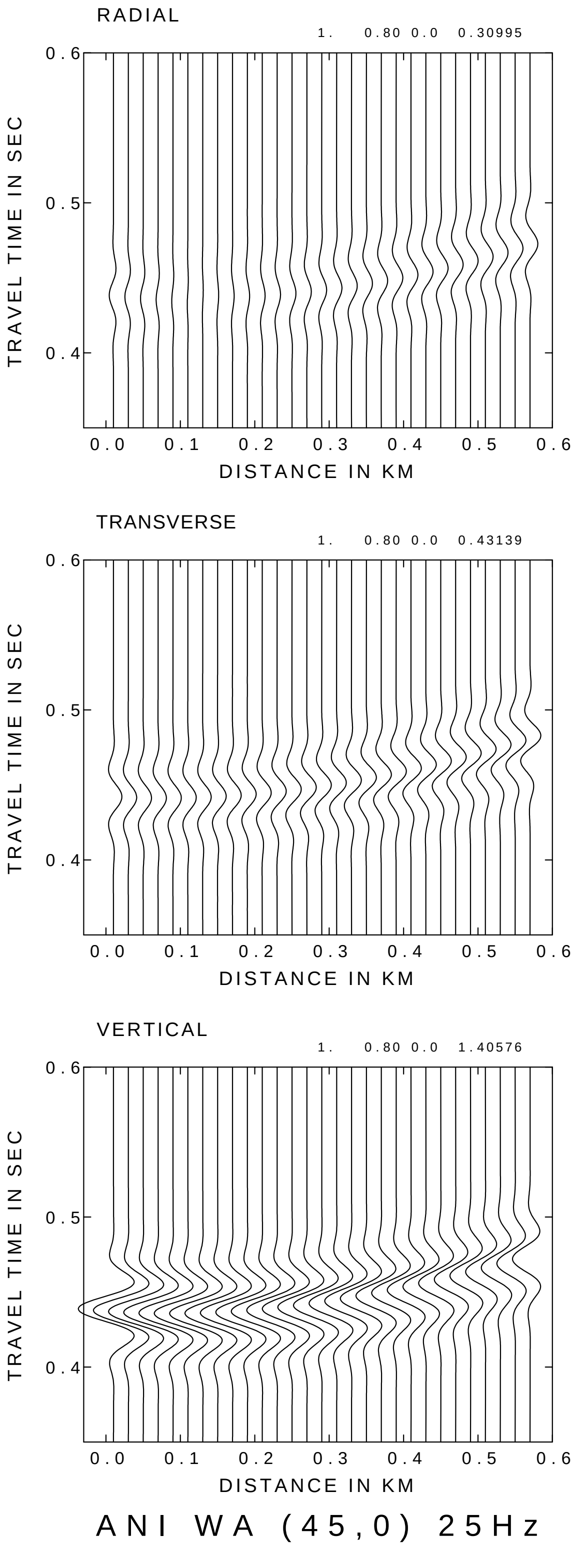
RADIAL
1. 0.80 0.0 0.30995
TRAVEL TIME IN SEC
DISTANCE IN KM
TRANSVERSE
1. 0.80 0.0 0.43139
TRAVEL TIME IN SEC
DISTANCE IN KM
VERTICAL
1. 0.80 0.0 1.40576
TRAVEL TIME IN SEC
DISTANCE IN KM
ANI WA (45,0) 25Hz

Figure 23

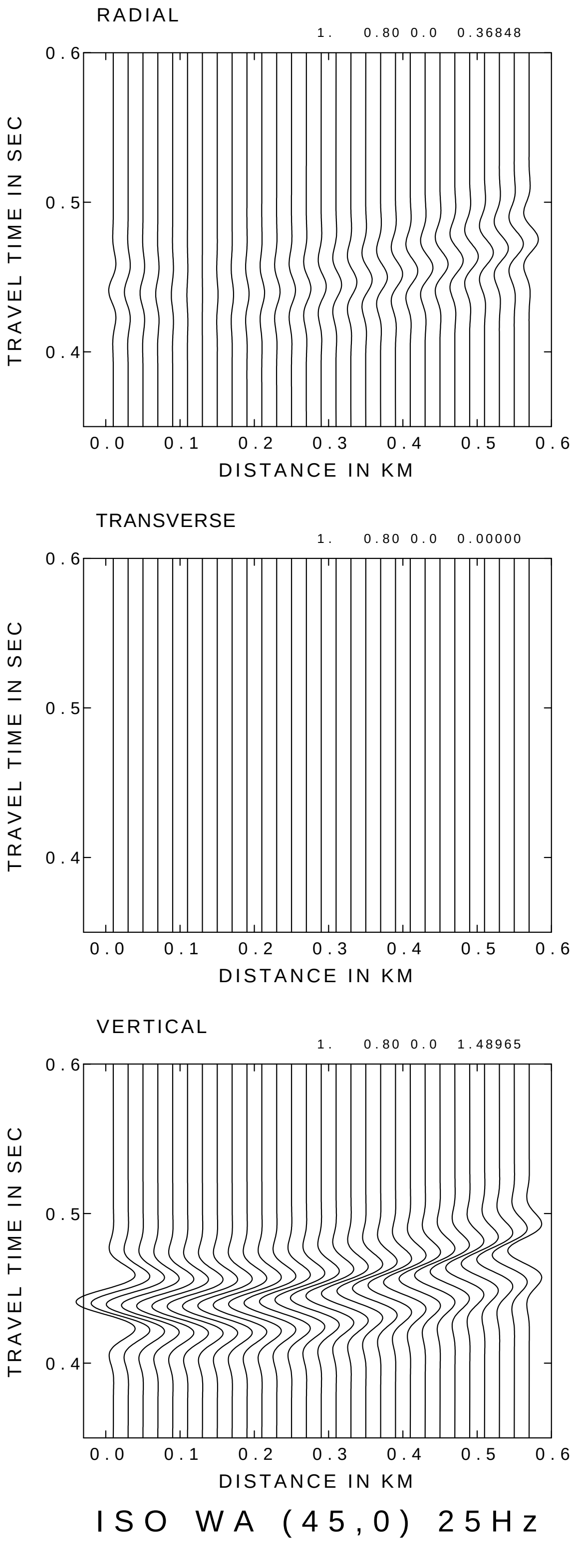
RADIAL
1. 0.80 0.0 0.36848
TRANSVERSE
1. 0.80 0.0 0.00000
VERTICAL
1. 0.80 0.0 1.48965
TRAVEL TIME IN SEC
0.6
0.5
0.4
0.0 0.1 0.2 0.3 0.4 0.5 0.6
DISTANCE IN KM
ISO WA (45,0) 25Hz

Figure 24

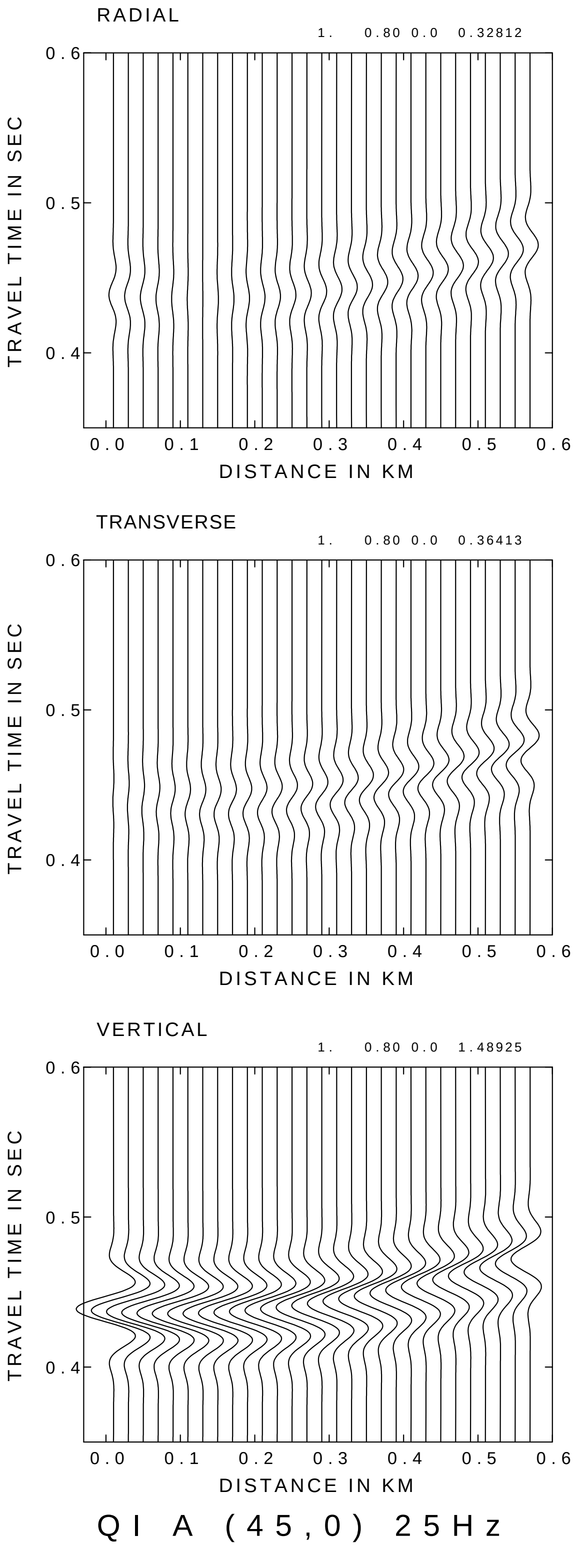
RADIAL
1. 0.80 0.0 0.32812
TRAVEL TIME IN SEC
0.6
0.5
0.4
0.0 0.1 0.2 0.3 0.4 0.5 0.6
DISTANCE IN KM
TRANSVERSE
1. 0.80 0.0 0.36413
TRAVEL TIME IN SEC
0.6
0.5
0.4
0.0 0.1 0.2 0.3 0.4 0.5 0.6
DISTANCE IN KM
VERTICAL
1. 0.80 0.0 1.48925
TRAVEL TIME IN SEC
0.6
0.5
0.4
0.0 0.1 0.2 0.3 0.4 0.5 0.6
DISTANCE IN KM
QI A (45,0) 25Hz

Figure 25

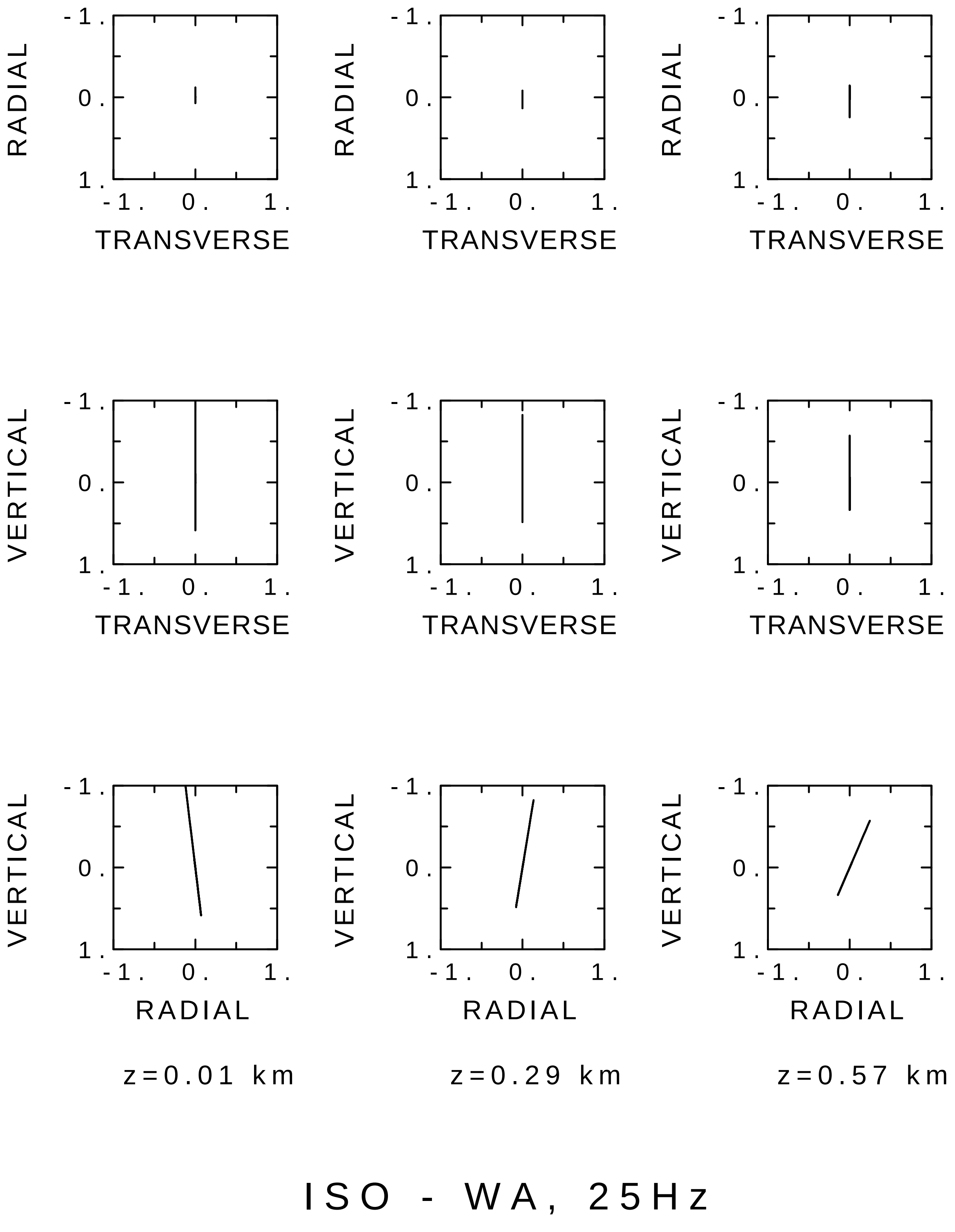
RADIAL
TRANSVERSE
VERTICAL
-1.
0.
1.
z=0.01 km
z=0.29 km
z=0.57 km
ISO - WA, 25Hz

Figure 26

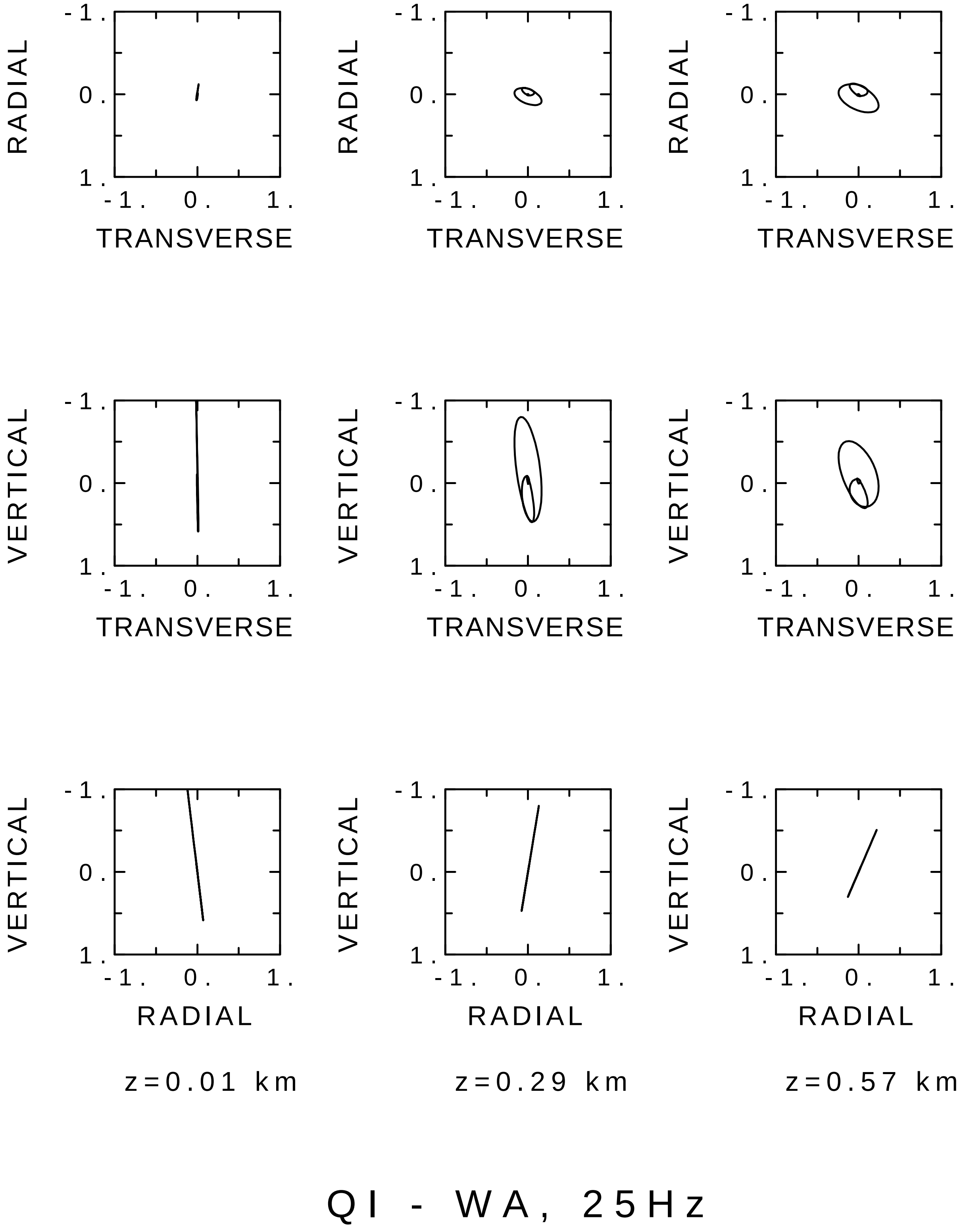
RADIAL
TRANSVERSE
VERTICAL
TRANSVERSE
VERTICAL
RADIAL
-1.
0.
1.
z=0.01 km
z=0.29 km
z=0.57 km
QI - WA, 25Hz

Figure 27

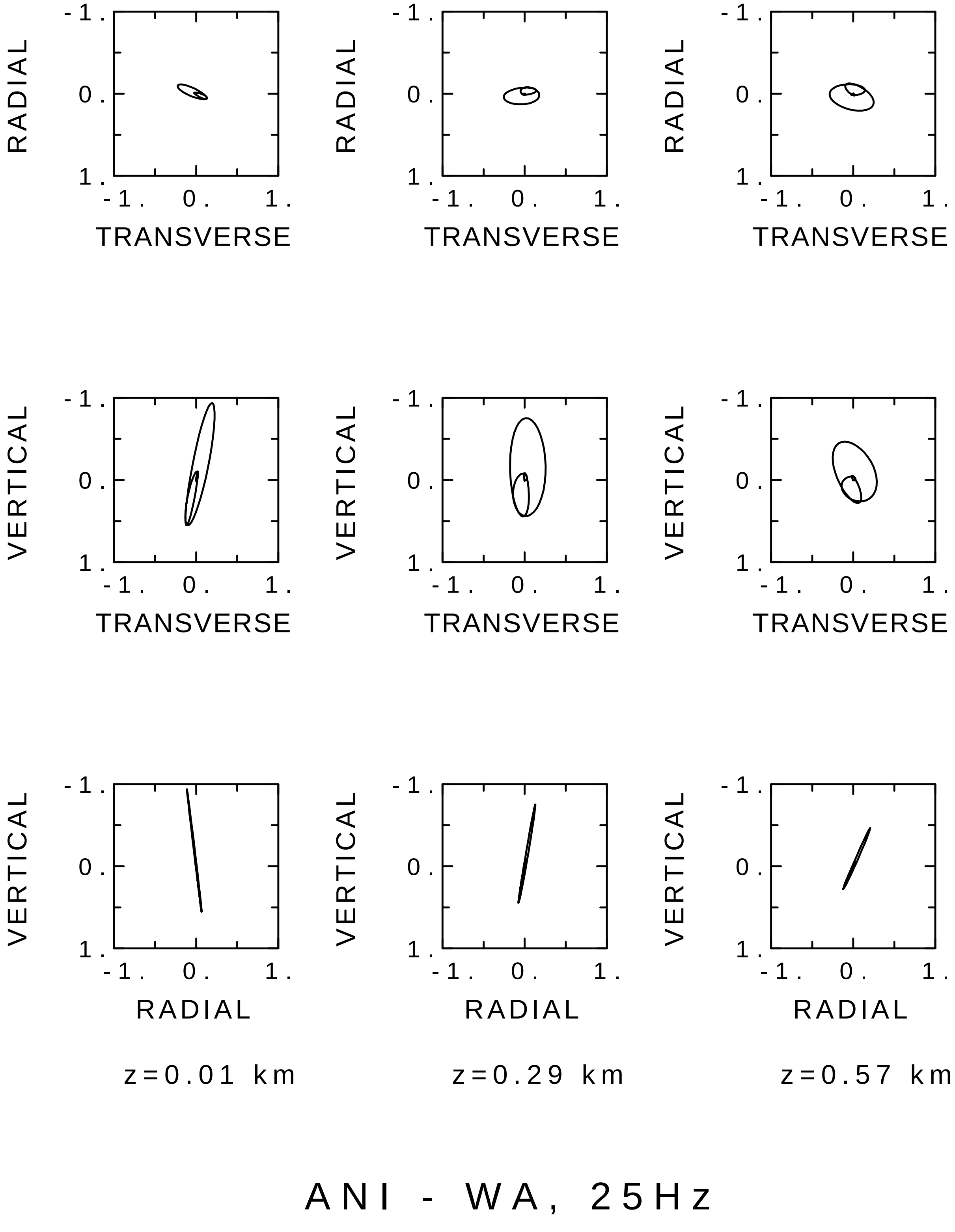

RADIAL
TRANSVERSE
VERTICAL
-1.
0.
1.
z=0.01 km
z=0.29 km
z=0.57 km
ANI - WA, 25Hz

Figure 28

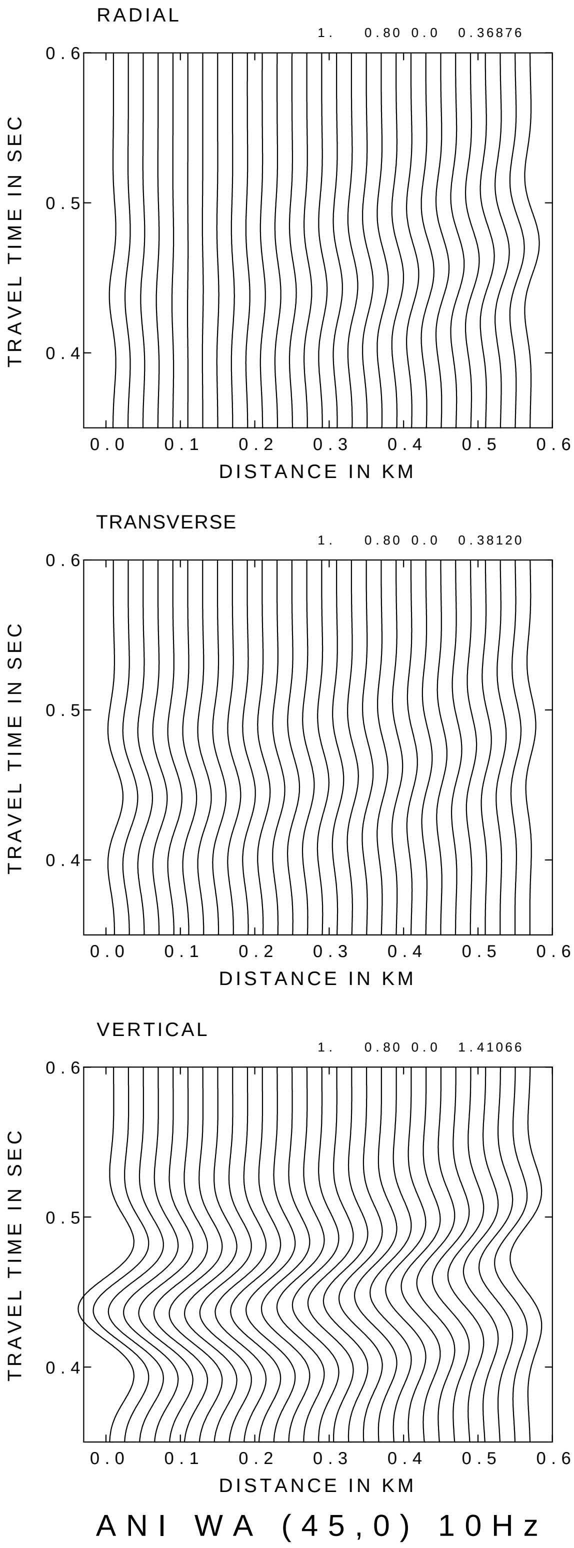
RADIAL
1. 0.80 0.0 0.36876
TRAVEL TIME IN SEC
0.6
0.5
0.4
0.0 0.1 0.2 0.3 0.4 0.5 0.6
DISTANCE IN KM
TRANSVERSE
1. 0.80 0.0 0.38120
TRAVEL TIME IN SEC
0.6
0.5
0.4
0.0 0.1 0.2 0.3 0.4 0.5 0.6
DISTANCE IN KM
VERTICAL
1. 0.80 0.0 1.41066
TRAVEL TIME IN SEC
0.6
0.5
0.4
0.0 0.1 0.2 0.3 0.4 0.5 0.6
DISTANCE IN KM
ANI WA (45,0) 10Hz

Figure 29

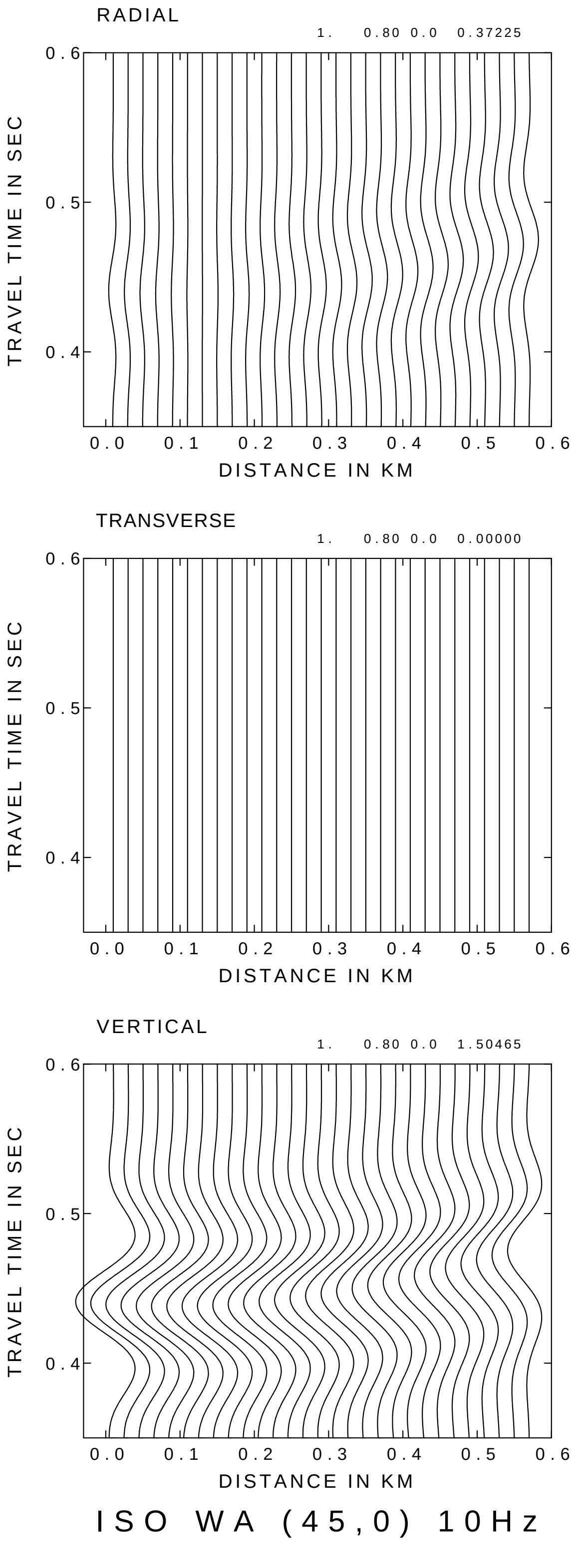
RADIAL
1. 0.80 0.0 0.37225
TRAVEL TIME IN SEC
0.6
0.5
0.4
0.0 0.1 0.2 0.3 0.4 0.5 0.6
DISTANCE IN KM
TRANSVERSE
1. 0.80 0.0 0.00000
TRAVEL TIME IN SEC
0.6
0.5
0.4
0.0 0.1 0.2 0.3 0.4 0.5 0.6
DISTANCE IN KM
VERTICAL
1. 0.80 0.0 1.50465
TRAVEL TIME IN SEC
0.6
0.5
0.4
0.0 0.1 0.2 0.3 0.4 0.5 0.6
DISTANCE IN KM
ISO WA (45,0) 10Hz

Figure 30

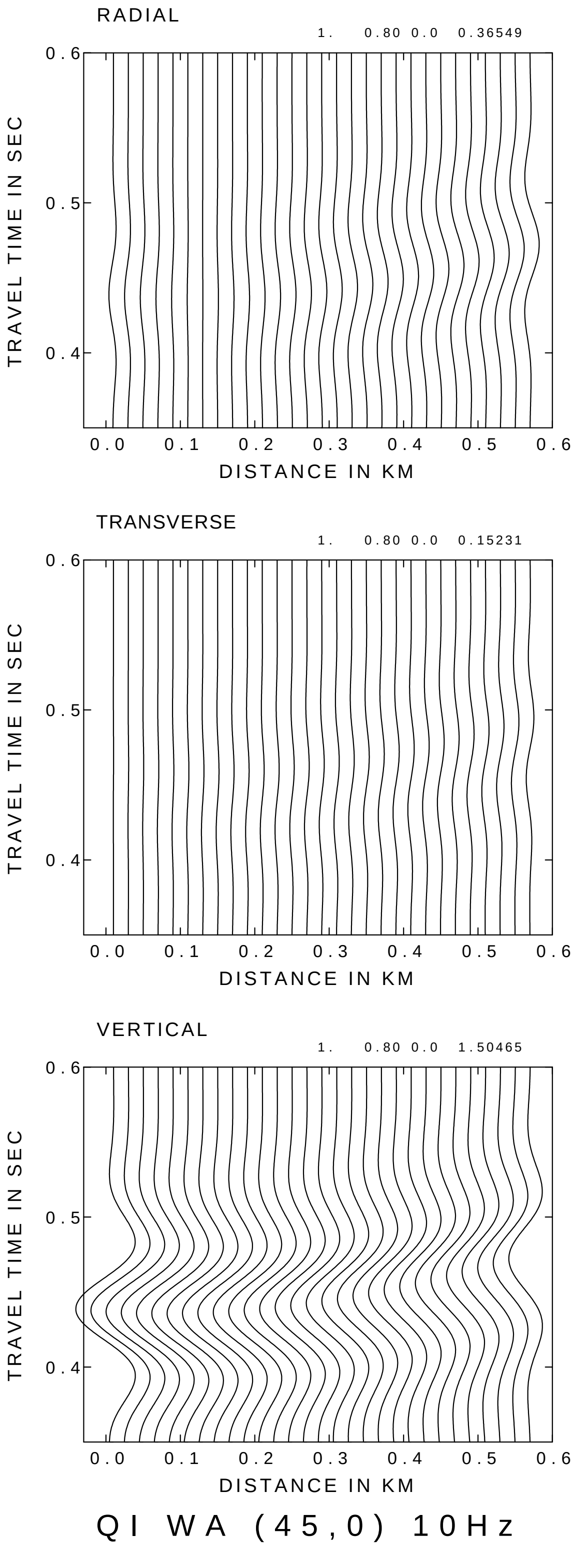

RADIAL
1. 0.80 0.0 0.36549
TRAVEL TIME IN SEC
DISTANCE IN KM
TRANSVERSE
1. 0.80 0.0 0.15231
TRAVEL TIME IN SEC
DISTANCE IN KM
VERTICAL
1. 0.80 0.0 1.50465
TRAVEL TIME IN SEC
DISTANCE IN KM
QI WA (45,0) 10Hz

Figure 31

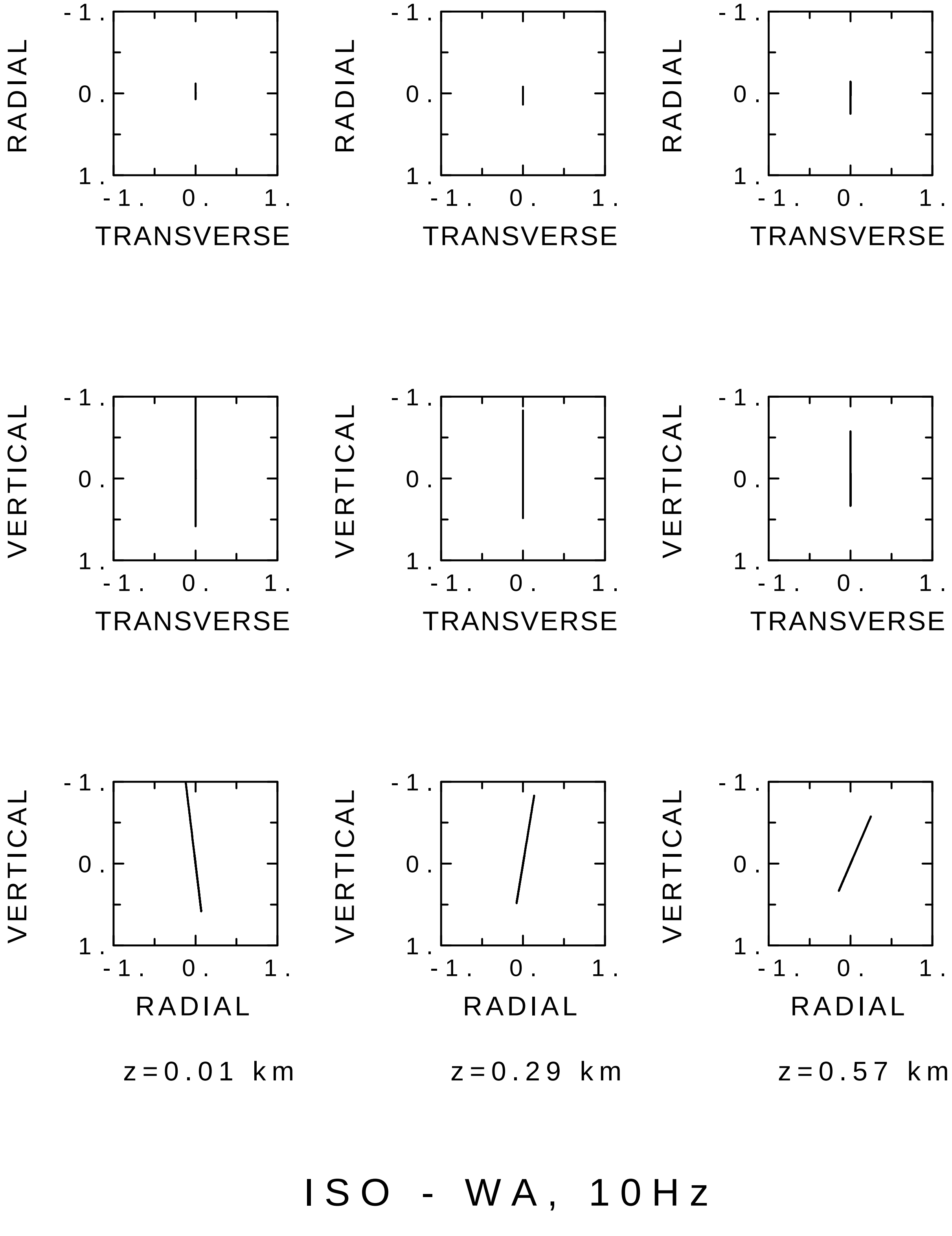
RADIAL
TRANSVERSE
VERTICAL
TRANSVERSE
VERTICAL
RADIAL
-1.
0.
1.
z=0.01 km
z=0.29 km
z=0.57 km
ISO - WA, 10Hz

Figure 32

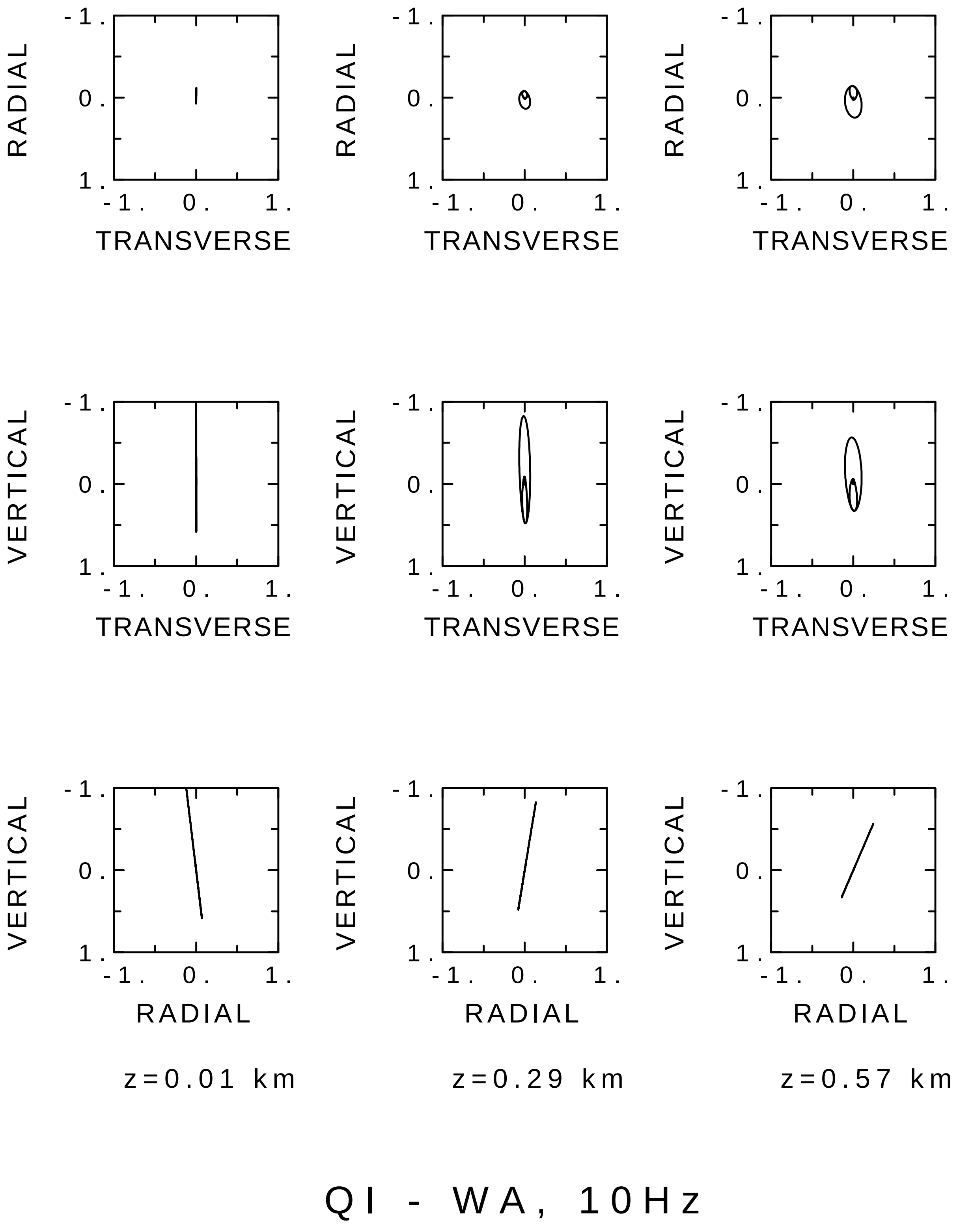
RADIAL
TRANSVERSE
VERTICAL
RADIAL
-1.
0.
1.
z=0.01 km
z=0.29 km
z=0.57 km
QI - WA, 10Hz

Figure 33

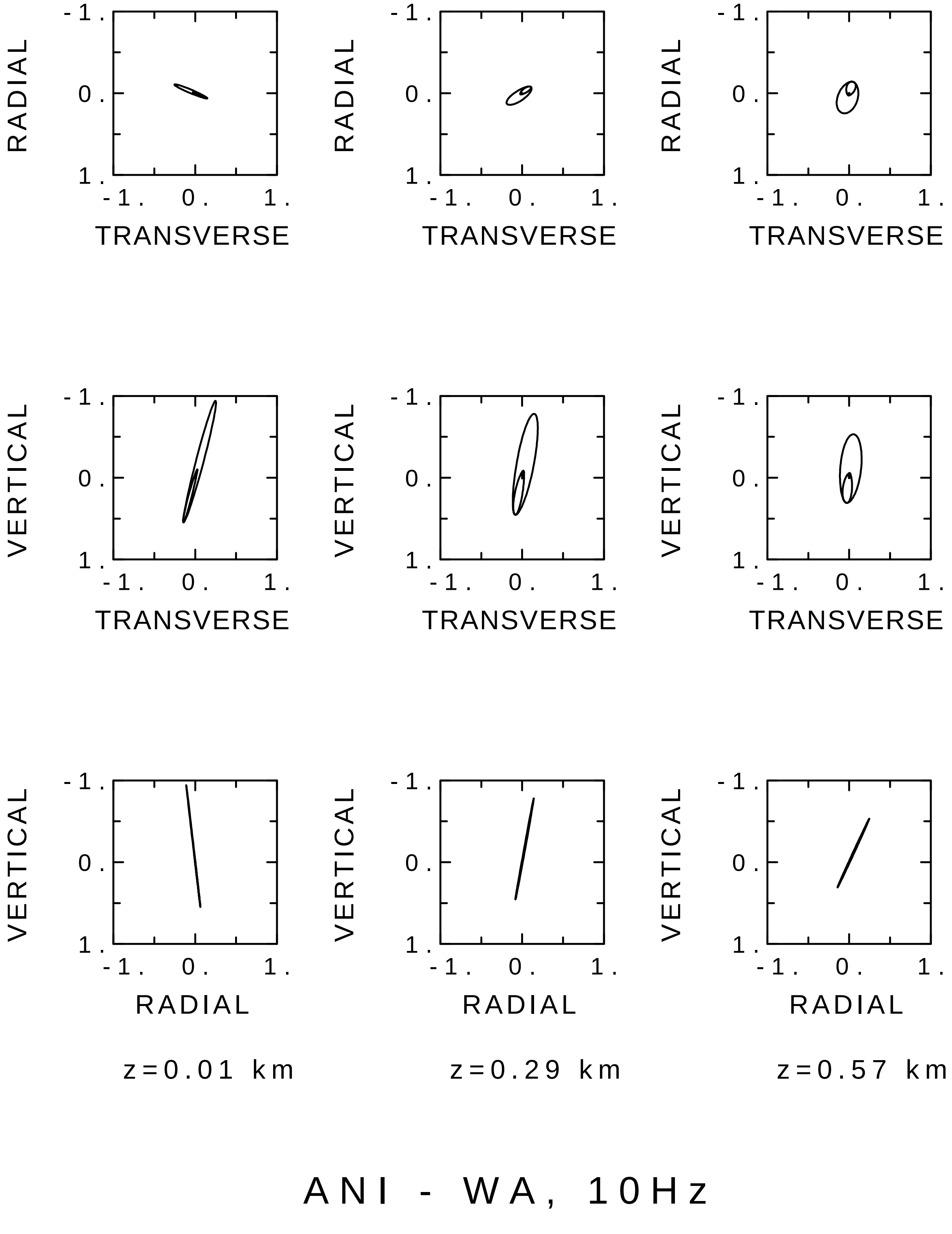
RADIAL
TRANSVERSE
VERTICAL
TRANSVERSE
VERTICAL
RADIAL
-1.
0.
1.
z=0.01 km
z=0.29 km
z=0.57 km
ANI - WA, 10Hz

Figure 34

ray methods. Between these limits, the zero-order approximation of the QI approach yields results describing coupling of the two qS waves, which can be obtained by zero-order approximations of neither of the ray methods. Quality of these results must be tested by comparing them with results of independent and more accurate methods.

The numerical tests showed the effects of frequency and strength of anisotropy on coupling or decoupling of qS waves. The qS waves decouple with increasing frequency and with increasing strength of anisotropy or, more precisely, with increasing separation of phase velocities of the qS waves and distance on which they propagate. Another important factor is inhomogeneity. Study of effects of inhomogeneity on coupling and decoupling of qS waves will be one of the next steps in the study of the QI approach.

All the above computations were performed only with the zero-order approximation of thew QI approach. The absence of the first-order additional terms did not seem to effect the results of the QI approximation very much, at least in the considered models. The effects of the first-order additional terms should be seen most strongly in the vertical - radial plane of particle motion diagrams in Figs.20 - 22. We can see, however, that the projections of the particle motion into this plane have practically identical orientation in all three figures. The considered anisotropy was probably weak to produce observable effects. Nevertheless, attempts will be made to introduce the first-order additional terms to the QI calculations.

The synthetic test on the EWA model showed that the QI approximation works well not only in regions of weak anisotropy but also in a singular region, specifically in a region of an intersection singularity. Applications of the QI approach in singular regions in media with a stronger anisotropy and comparison of QI results with results of other independent methods is another task for near future.

Another problem, which requires attention in a near future is the problem of a proper choice of the background isotropic medium and its effects on the quality of results of the QI approach.

All the results in this contribution were obtained for a single force source whose directivity is quite similar to the directivity of the same source in an isotropic medium. In future studies, other types of point sources with directivities more different from directivities in isotropic media will be also studied.

In this preliminary study, the QI approach was applied along the whole ray, from the source to the receiver. In future, we would like to use the QI approach in combination with the ray method. In regions where the qS waves couple, i.e. in regions of weak anisotropy or in singular regions, the QI approximation will be used while in regions, where the qS waves or an S wave propagate independently, the ray method will be used.

ACKNOWLEDGEMENTS

This work was supported by the consortium project "Seismic waves in complex 3-D structures (SW3D)", by the EC, INCO - Copernicus Project IC15 CT96 200 and by the Grant Agency of Czech Republic, Grant No. 205/96/0968.

REFERENCES

Bulant,P. & Klimeš, L., 1998. Coupling ray theory in weakly anisotropic media. In: Seismic Waves in Complex 3-D Structures, Report 7, Dept.of Geophysics, Charles University Prague, this issue.

Červený,V., 1998. Quasi–shear coupling in inhomogeneous weakly anisotropic media. Quasi–isotropic propagator matrices In: Seismic Waves in Complex 3-D Structures, Report 7, Dept.of Geophysics, Charles University Prague, this issue.

Coates,R.T. & Chapman,C.H., 1990. Quasi-shear wave coupling in weakly anisotropic 3-D media, *Geophys.J.Int.*, **103**, 301-320.

Kravtsov, Yu.A., 1968. "Quasiisotropic" approximation to geometrical optics, *Dokl. AN SSSR*, **183**, No.1, 74-77 (in Russian).

Kravtsov, Yu.A. & Orlov,Yu.I., 1980. *Geometrical optics of inhomogeneous media*, Nauka, Moscow (in Russian).

Pšenčík,I.,1997. Green functions for inhomogeneous weakly anisotropic media. In: Seismic Waves in Complex 3-D Structures, Report 6, pp.263-282, Dept.of Geophysics, Charles University Prague.

Pšenčík,I., 1998a. Green's functions for inhomogeneous weakly anisotropic media, *Geophys. J. Int.*, **103**, 279-288.

Pšenčík,I., 1998b. Package ANRAY, version 4.10 In: Seismic Waves in Complex 3-D Structures, Report 7, Dept.of Geophysics, Charles University Prague, this issue.

Pšenčík,I. & Gajewski,D., 1998. Polarization, phase velocity and NMO velocity of qP waves in arbitrary weakly anisotropic media. *Geophysics*, **63**, 1754-1766.